

ARIZONA GEOLOGICAL SOCIETY

SPRING FIELD TRIP

May



1982

Comparison of NASA Thematic Mapper images
of the Safford District with exposed alteration haloes
at the Phelps Dodge Dos Pobres and Kennecott Lone Star deposits

L.K. Lepley - Field Trip Leader

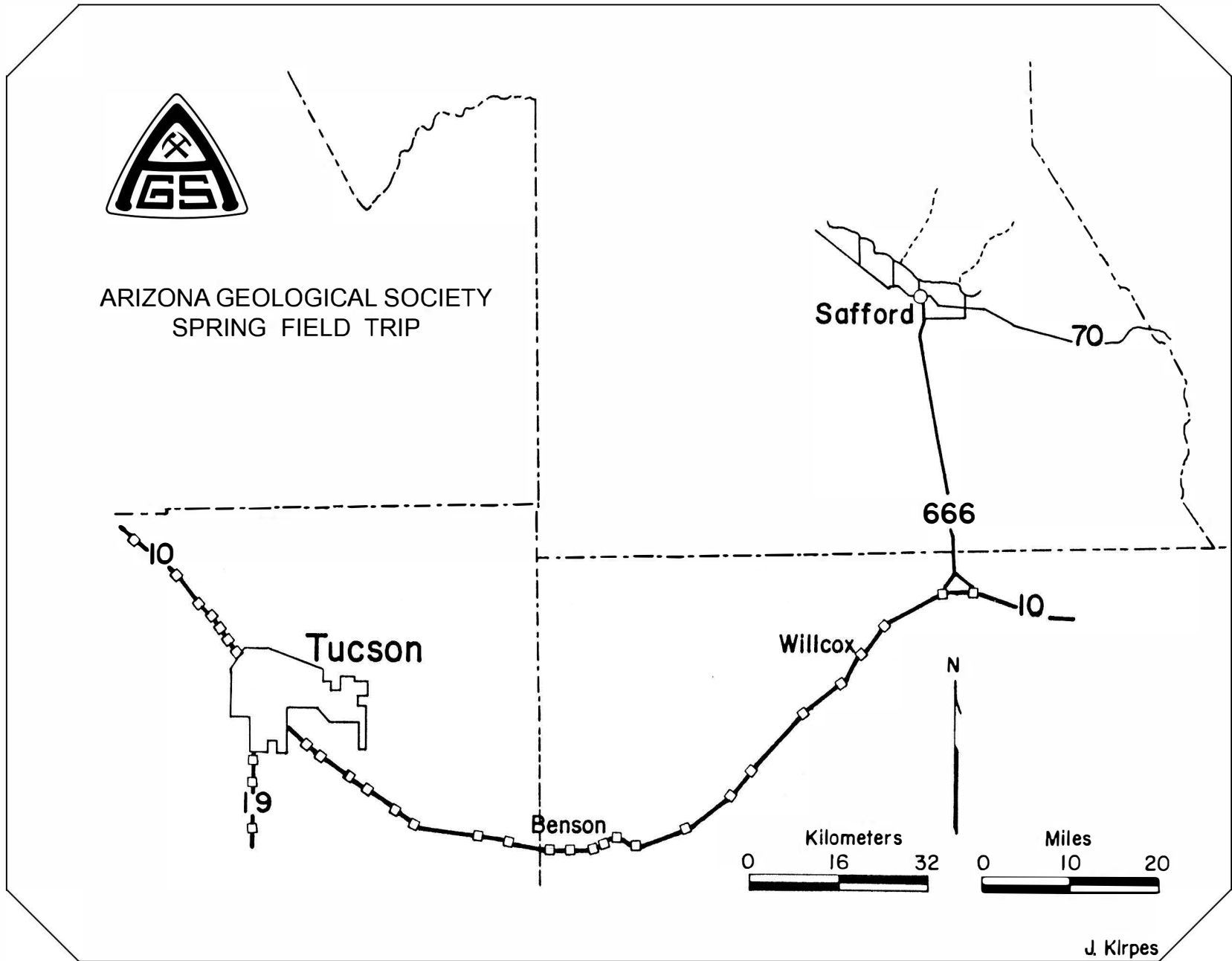


Figure 1. Road map, Tucson to Safford.

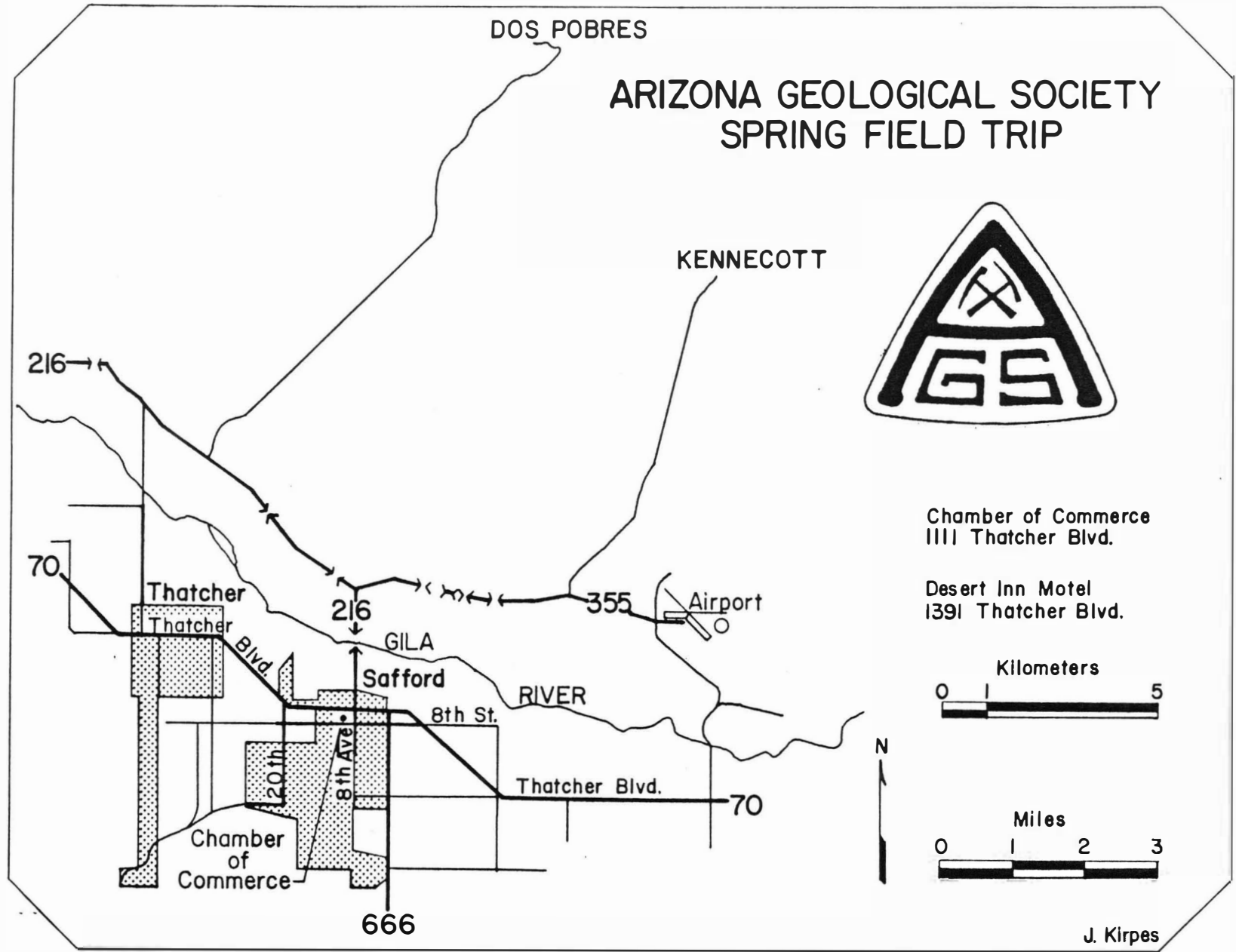


Figure 2. Road map, Safford and vicinity.

TABLE OF CONTENTS

Introduction	1
General Description of the Test Site	1
Geologic History	2
1. Stratigraphic Evolution	2
2. Structural Evolution	2
Landsat-D Thematic Mapper Application to Porphyry Copper Exploration	5
1. Introduction	5
2. Analysis of Landsat MSS Data	6
3. Analysis of Field Spectral Data	7
4. Thematic Mapper Simulator Aircraft Data	7
Rationale for Selection of the Safford Site.	9
Site-Specific Objective.	9
Remote Sensing Model	10
Data Sources and Interpretation Methods.	11
1. Remote Sensing Data	11
2. Support Data	12
3. Procedures for Interpretation and Comparison of Data	13
Image Processing	13
1. Contrast Enhancements	13
2. Banding Ratioing	14
3. Principal Components Analysis	14
4. Canonical Analysis	17
The Kennecott Deposit.	18
1. Lithology	18
2. Mineralization	18
3. Structure	18
4. Alteration	18
5. The NS-001 Canonical Transform Image and Its Interpretation	21

The Dos Pobres Deposit.	22
1. Lithology	22
2. Structure	23
3. Alteration	24
4. The NS-001 3-Ratio Image and Its Interpretation	28
Reflectance Spectra as Diagnostic Data.	29
1. Dos Pobres Spectra	30
2. Kennecott Spectra	30
References.	33

LIST OF TABLES

Table 1.	Spectral Bands of Landsat MSS and Landsat-D TM	6
Table 2.	Variance-Covariance Matrix for a Portion of a Landsat Image.	15
Table 3.	Eigenvalue Matrix after Principal Components Transformation for the Matrix in Table 2.	16
Table 4.	Eigenvector Matrix after Principal Components Transformation Based on Data of Tables 2 and 3.	16
Table 5.	Geologic Column and Geochronology of the Safford District.	32

LIST OF FIGURES

- Figure 1. Road map, Tucson to Safford
- Figure 2. Road map, Safford and vicinity
- Figure 3. Geologic map, Safford district (from P. Dunn, 1978)
- Figure 4. Cross sections, Safford district (from P. Dunn, 1978)
- Figure 5. Geologic map, vicinity of Kennecott deposit, 1:24,000 scale (courtesy of Bear Creek Mining Co., Kennecott Corp.)
- Figure 6. Legend for the Kennecott geologic map, Figure 5
- Figure 7. Map of mineralization distribution, vicinity of Kennecott deposit (courtesy of the Kennecott Corp.)
- Figure 8. Legend for the Kennecott map of mineralization, Figure 7
- Figure 9. Structural map, vicinity of the Kennecott deposit (courtesy of the Kennecott Corp.)
- Figure 10. Legend of the Kennecott structural map, Figure 9
- Figure 11. Enlarged portion of a NASA color aerial photograph of the Kennecott area, 1:24,000 scale
- Figure 12. Simulated Thematic Mapper image of the Kennecott area, 1:24,000 scale. This is a canonical transform image processed by the Jet Propulsion Laboratory from NASA NS-001 airborne scanner data (courtesy of the Geosat Committee, Inc.)
- Figure 13. Map of spectral anomalies, derived from the canonical transform image, indicating areas of suspected phyllic alteration. The location of samples taken for reflectance spectra and mineralogic analysis shown by numbers 1, 2, 3, and 4.
- Figure 14. Alteration map, vicinity of the Kennecott deposit, 1:24,000 scale (courtesy of the Kennecott Corp.)
- Figure 15. Legend for the Kennecott alteration map, Figure 14
- Figure 16. Enlarged portion of a NASA color aerial photograph of the Dos Pobres area, approximately 1:1,000,000 scale
- Figure 17. Geologic map of the vicinity of the Dos Pobres orebody, approximately 1:10,000 scale (courtesy of the Phelps Dodge Corp; also in Langton and Williams, 1982). Stipples indicate pervasive biotite alteration and disseminated cuprite-chrysocolla.
- Figure 18. Thematic Mapper Simulator image, three-ratio color composite image processed by Jet Propulsion Laboratory from NASA NS-001 multispectral data (courtesy of the Geosat Committee, Inc.)

- Figure 19. Map of spectral anomalies derived from the three ratio image, indicating areas of suspected phyllic alteration and the location of rock samples taken for analysis.
- Figure 20. Linear contrast stretch
- Figure 21. Elliptical scatter pattern and new set of coordinate axes
- Figure 22. Mean values and density distribution for hypothetical categories
- Figure 23. Canonical transform involving rotation and translation for categories
- Figure 24. Canonical rotation, translation, and scaling transformation
- Figure 25. Reflectance spectra of host rocks, showing positions of Thematic Mapper bands. Note the contrast between argillized (phyllic) rocks and propylitically altered rocks.
- Figure 26. Reflectance spectra of host rocks. Note the difference between spectra of weathered and fresh rock surfaces.

COMPARISON OF NASA THEMATIC MAPPER IMAGES OF THE SAFFORD DISTRICT
WITH EXPOSED ALTERATION HALOES AT THE PHELPS DODGE DOS POBRES
AND KENNECOTT LONE STAR DEPOSITS

INTRODUCTION

The purpose of this field trip is to allow the participants to examine images derived from an aerial multispectral scanner designed to simulate the Thematic Mapper to be included on the future Landsat D satellite. The participants can ground check the images to judge for themselves the effectiveness of the new spectral bands at 1.6 and 2.2 microns and of the digital processing of the data.

The first part of this guide reviews the Geosat/NASA/JPL Thematic Mapper simulator data pertaining to the exposed alteration haloes of the Kennecott and Dos Pobres deposits. Only the mineralogical aspects of the remote sensing are discussed here.

GENERAL DESCRIPTION OF THE TEST SITE

The Safford test site is located in Graham County, southeast Arizona. Major access to the region is provided by US Highway 70 from the northwest, and Interstate Highway 10 and US Highway 666 from the south and west. These highways intersect at the town of Safford, about 10 miles southwest of the mining district (figures 1 and 2).

The deposits studied are in the Safford (or Lone Star) district on the southwest flank of the Gila Mountains, one of several northwesterly-trending ranges characteristic of the Basin and Range physiographic province of southeastern Arizona. This range is on the eastern side of the Mountain Region or Mexican Highlands that separates the Colorado Plateaus province from the Sonoran Desert (Robinson and Cook, 1966). The area has one major drainage area, the Gila River, which runs from a southeasterly to a northwesterly direction; Bonita Creek drains the north part of the area and flows into the Gila River northeast of Safford. Several streams flow intermittently from the Gila Mountains in a southwest direction and join the Gila River.

Four separate porphyry copper deposits occur within a narrow northwest-trending belt along the southwestern flank of the Gila Mountains. From the northwest to southeast these are the Dos Pobres orebody,

operated by Phelps Dodge; the San Juan open pit operation leased by the Phalen Oil Company; the Safford deposit operated by Kennecott; and the Sanchez deposit held by Inspiration Copper.

GEOLOGIC HISTORY

1. *Stratigraphic Evolution.* Except for small xenoliths of Precambrian quartzite and Pleistocene-Recent deposits, the geologic column of the district consists of extrusive and intrusive igneous rocks. Table 1, modified after Langton and Williams (1982), summarizes the geologic history of the region. The older Safford metavolcanic series, in which the four separate porphyry copper deposits occur, consists of dark gray massive porphyritic andesite and fine-textured flow breccia with intercalated tuff beds.

These older Safford volcanics are overlain unconformably by the intermediate Baboon metavolcanic series consisting of dacite, andesite, latite, flow breccia and tuff.

The younger Gila Mountain volcanic series, consisting of basalt flows, tuff, and agglomerate, disconformably overlies the intermediate Baboon volcanic series. The premineral Safford metavolcanic rocks have been intruded by the Lone Star quartz-diorite pluton, a representative of the underlying parental magma from which the metavolcanics were derived. The disseminated copper mineralization is associated with stocks of quartz monzonite porphyry, exposed at the San Juan, Sanchez, and Dos Pobres deposits and encountered at depth at the Kennecott deposit.

The andesite and comagmatic quartz diorite plutons have been cut by latite and quartz latite dikes in northeast-trending swarms. By P. Dunn's (1978) interpretation, the latite dikes are related to the quartz diorite, and the quartz latite dikes are related to the mineralizing quartz monzonite porphyry stocks.

A large near-vertical pipe of mineralized tuff is partially exposed near the center of the Kennecott deposit. Gently dipping beds suggest a collapse origin by removal of magma at depth (P. Dunn, 1978).

The postmineral volcanic rocks of the district can be divided into three units: upper Eocene hornblends andesite dikes, sills and plugs; Miocene-Pliocene siliceous tuffs, rhyolite and agglomerates; and late Pliocene basalt flows and interbedded tuffs.

2. *Structural Evolution.* Analogous to the Morenci-Metcalf district 32 km to the northeast, the major fault zones strike N-S, ENE-WSW, and NW-SE. The northwest faults are parallel to the elongated regional structural belt, conceivably part of an older right-lateral system. Elongation of the premineral

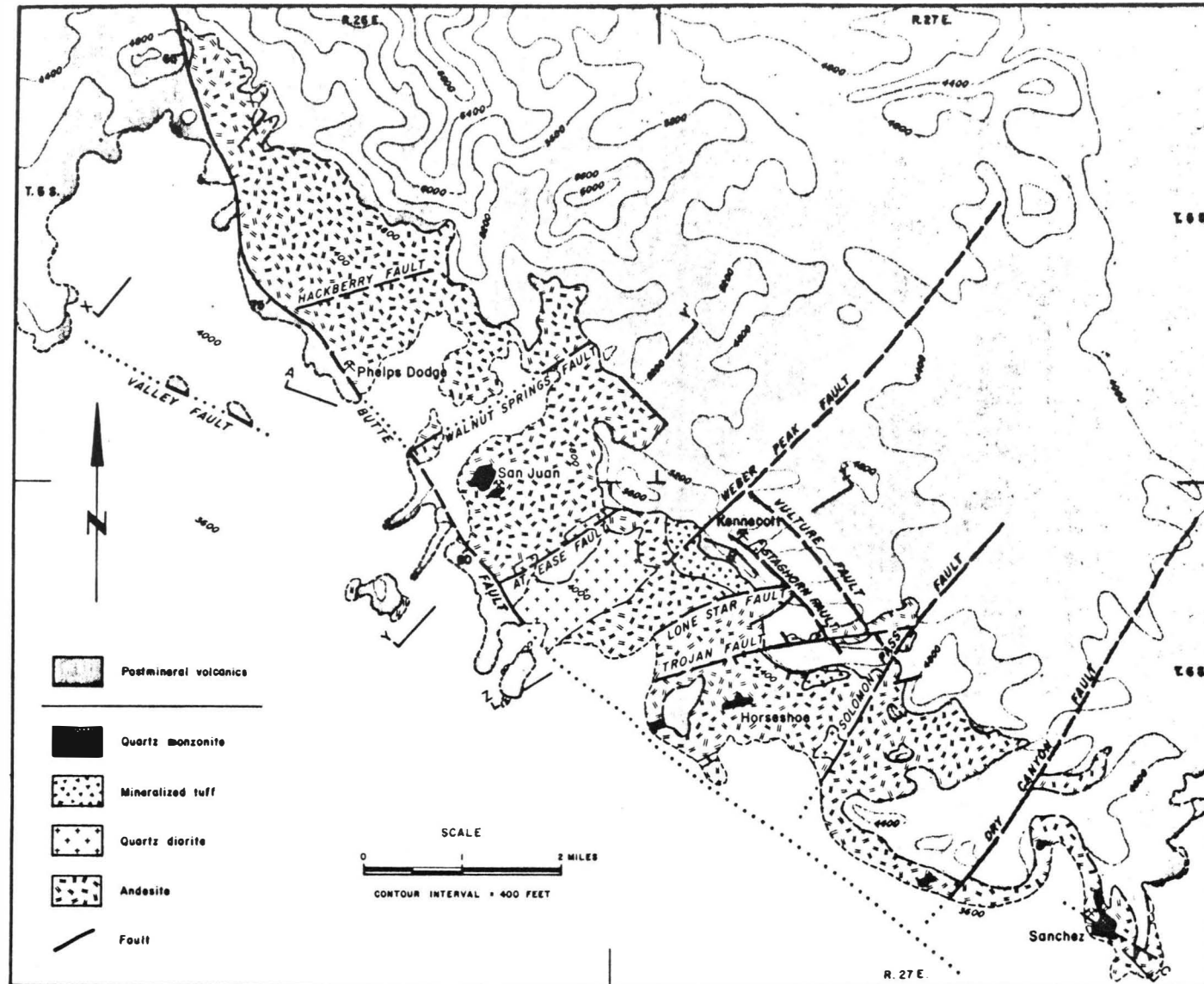


Figure 3. Geologic map, Safford district (from P. Dunn, 1978).

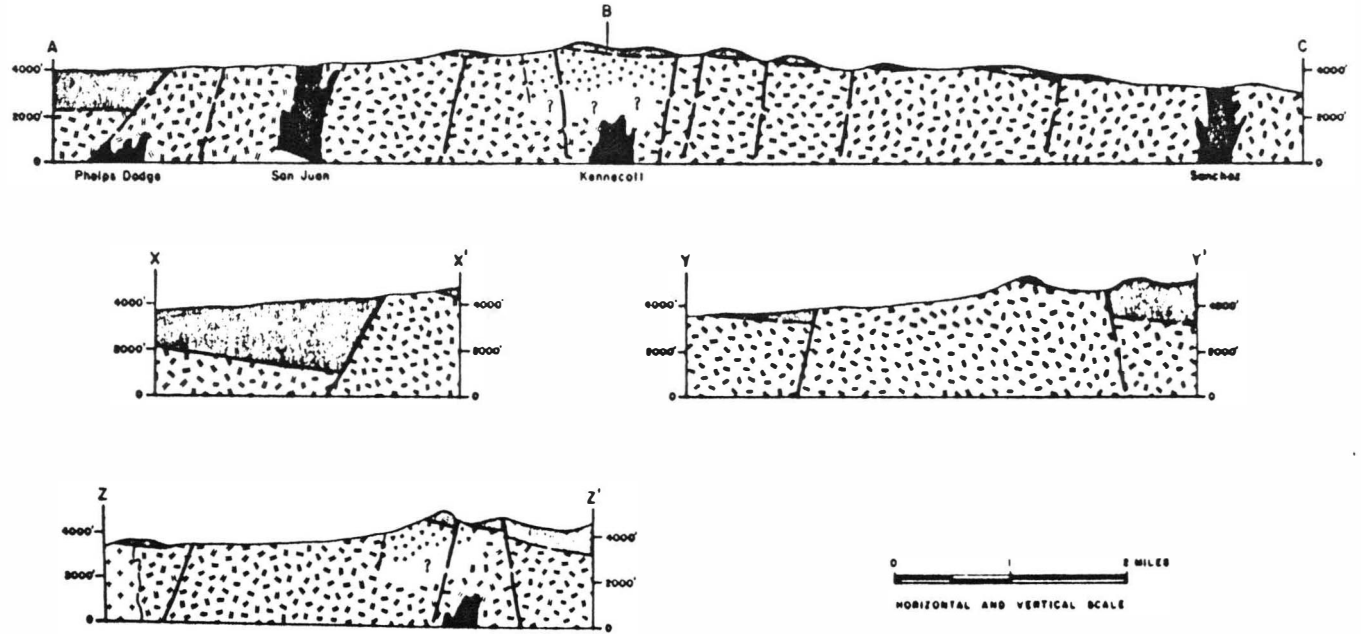


Figure 4. Cross sections, Safford district (from P. Dunn, 1978).

outcrop belt and irregular alignment of quartz monzonite porphyry stocks within the district are both thought to be a reflection of the same regional structures that controlled the northwest-trending faults.

The most prominent structural features at the porphyry deposits are northeast to east-northeast mineralized fractures and dikes. At least six major northeast-striking faults cut the premineral andesite: the Lone Star, Trojan, Weber Peak, Dry Canyon, Solomon Pass, Walnut Springs, and Hackberry faults (P. Dunn, 1978). The northeasterly faults apparently controlled the present location of the porphyry copper deposits. Copper mineralization along the Lone Star, At Ease, and Hackberry faults indicates their early existence. The apparently comagmatic productive quartz monzonite stocks at the four porphyry copper deposits seem to have been displaced vertically 500 to 750 meters by early Tertiary movements along these northeasterly faults (see figure 4). These northeast fractures and faults are a regional feature common in many of the Laramide stocks in Arizona (Rehrig and Heidrick, 1972).

Northwest-southeast en echelon faults are the most pronounced features in the district. Reactivation by gravity movement since Miocene time has offset the Butte fault approximately 1,000 meters vertically. Postmineral vertical displacement on the other northwest-striking faults is no more than 100 meters. The displacement of marker units within the volcanic units indicates that these faults were reactivated during the postmineral volcanism (see cross sections, figure 4).

LANDSAT-D THEMATIC MAPPER APPLICATION TO PORPHYRY COPPER EXPLORATION

(Part of the following description of the Geosat/NASA/JPL evaluation of the Thematic Mapper test cases was extracted verbatim from Abrams, M., D. Brown, L. Lepley, and R. Sadowski (1982), attached as an appendix to this Field Guide.)

1. *Introduction.* Landsat data have been used for a number of years in arid to semi-arid environments to locate areas of iron oxide occurrences which might be associated with hydrothermal alteration zones. Pioneering work by Rowan and his coworkers in 1974 clearly demonstrated the utility of computer processing of Landsat data to locate alteration zones in Nevada associated with precious metal deposits. However, iron oxides have a wide range of occurrences often unrelated to alteration phenomena; these include sedimentary redbeds, volcanic rocks, weathered alluvium, etc. In addition there are areas of alteration which are iron-oxide free, such as advanced argillic, silicic, and solfataric alterations. These areas are

characterized by the presence of hydrous minerals, such as kaolinite, alunite, and sericite. The spectral information provided by the current Landsats does not allow detection of these areas, and fails to distinguish many unaltered areas from altered areas. Another drawback of the Landsat is its relatively poor spatial resolution (80 m) which prevents recognition of moderate to small features and outcrops which might be of critical importance.

The fourth Landsat, scheduled to be launched in July, 1982 will carry a new-generation multispectral scanner called the Thematic Mapper (TM). This instrument will have 7 channels to provide data with 30 m spatial resolution (Table 1).

TABLE 1. SPECTRAL BANDS OF LANDSAT MSS AND LANDSAT-D TM

Landsat MSS		Landsat-D TM	
<u>Band</u>	<u>Wavelength</u>	<u>Band</u>	<u>Wavelength</u>
4	0.5-0.6	1	0.46-0.50
5	0.6-0.7	2	0.52-0.60
6	0.7-0.8	3	0.63-0.69
7	0.8-1.1	4	0.76-0.90
		5	1.55-1.75
		6	2.08-2.36
		7	10.80-12.50

Two of the spectral channels (1.6 μm and 2.2 μm) are located in wavelength regions which should allow detection of hydrous minerals as well as iron oxides, using data from the other bands.

To examine the applications of Landsat-D TM data for copper exploration, Landsat data were compared with simulated TM data acquired using an aircraft scanner instrument. Three porphyry copper deposits in Arizona were selected for investigation: Silver Bell, Safford, and Helvetia. These sites present a range of copper occurrences in semi-arid environments, with different host rocks, levels of erosion, and stages of development. Both sedimentary and igneous terrains are represented; the varying levels of erosion provide exposures of alteration phenomena from the most intense potassic to regional propylitic.

2. *Analysis of Landsat MSS Data.* Landsat data provided some information on alteration at all three sites. Using a color ratio composite of band ratios 4/5, 5/6, and 6/7 areas with iron oxides present at the surface were identifiable at all sites. These areas include both altered rocks and iron-rich unaltered

rocks. At Silver Bell, iron oxides associated with the phyllic alteration zone along the Silver Bell fault zone were identifiable. Other, unaltered areas have a similar appearance on the images, including sedimentary redbeds and limonitic Precambrian granites. A few rock types were separable, but the limited spatial and spectral resolution made discrimination of many rock types impossible. At Safford, iron oxide areas associated with two copper deposits were identifiable; additional areas of iron oxide corresponding to weathered alluvium and gravels appeared similar. At Helvetia, altered hematitic arkose was discernible as were areas of unaltered volcanic sediments. Again, the poor spatial and spectral resolution provided only limited geologic information.

3. *Analysis of Field Spectral Data.* In order to examine the expected improvement provided by the Landsat-D TM spectral data, field reflectance measurements were obtained using JPL's Portable Field Reflectance Spectrometer (PFRS) at the three test sites. Most of the major rock types at the sites were measured in the wavelength region of 0.45 to 2.45 μm . Statistical analyses of the spectra were performed using a stepwise linear discriminant analysis program. The program was provided groups of rock spectra, and various wavelength regions from the PFRS data simulating several scanners. The program determined the optimal linear combination of the wavelength variables to separate the rock-type groups.

In a comparison of the separability of groups from each of the test sites for Landsat MSS and simulated Landsat-D TM data, the TM data provided an increase of about 20% in correctly identified sampled rock groups in all three test sites.

For retrospective verification and explanation of spectral anomalies mapped by the TM simulator aircraft scanner, laboratory reflectance spectra and XRD analyses were obtained from rock samples collected at the sites of these anomalies. The results of these analyses are discussed below under Safford Test Site.

4. *Thematic Mapper Simulator Aircraft Data.* Thematic Mapper data were obtained with NASA's NS-001 TM simulator aircraft scanner. Data were obtained from an altitude of 5 km, producing a 10 km swath width with a resolution of about 12 m. This scanner has the same 7 bands as the TM, and an additional band at 1.0-1.3 μm .

In order to examine detection of hydrothermal alteration, a color ratio composite was produced for each of the three sites using TM band ratios 3/2 (0.66 μm /0.56 μm), 4/5, and 5/6 (1.6 μm /2.2 μm). These particular ratios were chosen to enhance the presence of iron oxide minerals and hydrous minerals. The

3/2 ratio will be high for iron oxides due to the fall off in reflectance towards the ultraviolet. Hydrous minerals will have a high 5/6 value due to the absorption band near 2.2 μm caused by OH^- . This particular combination was shown to be effective for discriminating hydrothermal alteration of an epithermal precious metal deposit in Nevada.

At Silver Bell, the phyllic alteration zone was clearly delineated. Comparison with an alteration map produced from months of field and laboratory work showed a nearly perfect correlation. This zone was distinguishable due to spectral features of the mineralogical constituents. Iron oxides (goethite, hematite) developed on the surface from oxidation of hydrothermal pyrite, and kaolinite and sericite produced from alteration of feldspars, have diagnostic and strong absorption features in the TM wavelength bands. Sedimentary redbeds and other ferruginous, unaltered rocks were distinguishable from altered rocks due to their lack of hydrous minerals.

At Safford, sericitic alteration associated with the copper deposits showed up clearly for the same reasons as at Silver Bell. The altered rocks were a quartz monzonite intrusive, and rhyolitic dikes along a shear zone. At Helvetia, a large hematitic area east of the ore body was visible. This area has pervasive hematite developed from oxidation of hydrothermal pyrite. Argillic alteration was discernible over an outcrop of the mineralizing quartz latite porphyry.

The NS-001 TM data were also processed using stepwise linear discriminant function analysis. The ground spectral reflectance measurements provided the training sets to calculate the optimal linear combination of wavelength bands to separate the rock groups examined.

For Silver Bell, analysis of the images produced from the new linear combinations indicated that all the mapped geologic units could be distinguished. In addition, some of the mapped units appeared in different colors, corresponding to phyllic and propylitic alteration, and unaltered rocks. These data were degraded to the Landsat-D resolution of 30 m; little information was lost compared to the original 12 m data. Major dikes were visible, allowing structural information to be extracted; all outcrops were separable.

Similar processing was performed on the Safford and Helvetia data, with equally successful results. At Helvetia, unaltered limestones were separable from altered limestones (marbles) related to skarn development. The overall improvement compared to current Landsat data was striking.

RATIONALE FOR SELECTION OF THE SAFFORD SITE

The Safford (Lone Star) district was chosen because it contains three known deeply buried porphyry copper deposits. Only minor outcrops of the mineralizing intrusives show at the surface, and surface alteration is mainly limited to the outer zones of a typical porphyry copper deposit. The center of one deposit, Kennecott's Safford deposit, is covered by a postmineral lava flow. Another deposit, Dos Pobres, is not only deeply buried, but is split by a normal fault. The down-faulted block is now covered by several hundred meters of alluvium. Extensive postmineral volcanic rocks cover the Kennecott deposit. In contrast to the well-exposed Silver Bell site, only the outer fringes of the alteration associated with the buried deposits are exposed. This represents the present real-world situation in exploration for concealed deposits.

Vegetation cover and cultural disturbances are minimal. Access to one of the deposits and unpublished maps and reports were made available by Phelps Dodge Corp., a Geosat member. Published information on the district and on the Kennecott deposit shows that the area has been well studied and contains typical porphyry copper deposits (Dunn, 1978; Robinson and Cook, 1966.)

SITE-SPECIFIC OBJECTIVES

The overall objective of the Safford test site study is to assess the usefulness of a number of remote sensing systems as mapping tools in a known porphyry copper environment. The various imaging systems, alone and in combination with each other, have been evaluated in their ability to remotely discriminate the major rock types, alteration patterns, and structural elements associated with porphyry copper mineralization of several major deposits. The major observable features include:

1. Phyllic Alteration: definition of the phyllic alteration that represents the outer zones of the known buried deposits in the district.
2. Peripheral Alteration: identification of alteration areas associated with hydrothermal activity in other parts of the district.
3. Rock Types: discrimination of the main lithologies in the area, based on their individual spectral characteristics.
4. Structural Features: identification of major structural elements, including regional

northwest faults (Butte, Valley, etc.), transverse faults, and ENE prophyry dike swarms.

REMOTE SENSING MODEL

The primary part of our remote sensing model is the spectral modeling features expected to be observable through images obtained from three scanner devices including (1) Landsat 4-channel MSS, (2) M²S 11-channel scanner, and (3) Landsat-D Thematic Mapper as simulated by the NS-001 scanner. An idealized, synthetic, 30-channel array was also evaluated from a theoretical point of view.

For comparison, a photogeologic model based on conventional color aerial photography is also considered. This model is limited by the by the availability of only three broad spectral bands available to color film and to the human eye. However, more textural, morphological, and other spatial information is available from the high spatial resolution of photographic film.

1. *Ore Zones.* The ore zones are not exposed in the Dos Pobres and Kennecott deposits. However, the mineralizing intrusions, the structures controlling the locus of intrusions and the mineral emplacement, and the intermediate and outer alteration zones are partially exposed.

2. *High-Pyrite Zones.* The "pyrite halo" at the Kennecott site consists of that portion of the main alteration zone outside of the main ore deposits. The pyritic zones are characterized by low copper concentrations, high pyrite/copper sulfide ratios, and relative abundances of jarositic limonite.

The presence of sericite and clay minerals in the pyritic zone tends to produce an overall lighter tone in contrast with the darker tones of surrounding fresh rocks. A diagnostic brick-red or yellowish-brown color is characteristic of the capping produced by oxidation of copper-poor sulfides.

3. *Phyllic/Argillic Alteration.* Phyllic and argillic alteration generally coincide with the pyritic zone, the general characteristics of which have already been summarized. In addition to the indirect tonal and geomorphic features, the main alteration minerals--sericite, clays, and limonite--can be detected directly by their diagnostic spectral absorption bands. The iron and hydroxyl absorption bands make phyllic and argillic alteration highly visible on both Landsat and aircraft imagery.

4. *Propylitic Alteration.* Areas of propylitic alteration should have an overall light tone and a pale greenish tint in the visible region of the spectrum, due to the presence of minerals such as albite, epidote, and chlorite. Also, the presence of small amounts of limonite from the oxidation of pyrite

should be detectable on Landsat and aircraft imagery. The Mesozoic andesite host rocks are pervasively propylitically altered by autometamorphism. The objective of the model, therefore, was to discriminate between propylitic and phyllic alteration. The propylitic zones would show less absorption in iron and hydroxyl bands.

5. *Plugs, Dikes, and Tuffs.* Eocene rhyolite, quartz latite, latite, and dacite plugs, dikes, and associated tuffs are exposed at the Kennecott property and north of the Phelps Dodge orebody. Some of these outcrops are hundreds of meters in length and width and should be visible against the andesitic Cretaceous-Paleocene metavolcanics.

6. *Productive Porphyries.* Paleocene-Eocene productive quartz monzonite, tonalite, and granodiorite porphyries are exposed at or near Dos Pobres, San Juan, and Kennecott. These generally contain abundant sericite and iron oxide and thus should be discernable with Thematic Mapper spectral bands.

7. *Structural Features.* Mineralization was controlled by northeast to east-northeast faulting that also controlled the emplacement of the productive porphyry stocks and dikes. The dike swarms and mineralized fractures and chemical zones were difficult to map by conventional methods because of the lack of marker units in the andesite. Because phyllic alteration follows these northeasterly structures, they should be mappable by their spectral contrast wherever the alteration zones are wider than the 10 meter resolution of the scanner.

The postmineral northwesterly Butte (Foothills) fault should be mappable from all sensors because it is marked by the contact between Tertiary alluvium against Mesozoic metavolcanics.

DATA SOURCES AND INTERPRETATION METHODS

1. *Remote Sensing Data.* Remote sensing data acquired for the Safford test site included aircraft radar, Landsat imagery, aircraft multispectral scanner data, and color aerial photography. This Field Guide discusses data from the NS-001 Thematic Mapper simulator acquired over Safford by NASA aircraft from Johnson Space Flight Center in October, 1978.

The NS-001 (TMS) scanner coverage consists of a west-northwest-oriented swath 30 x 11 km in size with an IFOV (instantaneous field of view) of 12 meters. Due to a brief malfunction of the NS-001 scanner, a 1.6-km-wide strip of data is missing from that swath. The missing 1.6 x 11 km strip is unfortunately

centered over the San Juan mine, so the remote sensing model was not tested over that area. The 11-channel data were acquired at a slightly higher altitude than the TMS data, and cover a northwest-oriented swath of 20 x 45 km with an IFOV of 15 m.

2. *Support Data.* Ancillary data used in the interpretation of the Safford images includes geological and geophysical information from both published and unpublished sources. Detailed geologic data on the Dos Pobres deposit and the surrounding area are provided by an unpublished Phelps Dodge geologic map at a scale of approximately 1:4,800. This map shows fine structural and lithologic details, including the location of the east-northeast mineralized shear zones, the Trans-Butte fault, the Dos Pobres anticline, the Red Dike fault zone, the contact between Cretaceous-Paleocene metavolcanic host rock and the nonmineralized Eocene Baboon metavolcanics, and most importantly the small (25 x 75 m) heavily altered Paleocene "productive" porphyry outcrops. This map was accompanied by an unpublished Phelps Dodge geologic report by J. M. Langton and S. A. Williams that has only now become available in published form (Titley, 1982).

The principal detailed geologic data for the entire Safford district was provided by three published 1:24,000 scale maps released by Bear Creek Mining Co. (Kennecott Corp.). These maps, compiled by Annan Cook in the early 1960's, include an alteration map, a geologic map, and a structure map. These maps showed the mineralized and altered east-northeast shear zones and productive porphyry dikes, the metavolcanic host rocks, the Lone Star parent pluton, and the outline of the phyllic alteration zone.

It is important to note that these Kennecott maps were compiled many years before the Geosat Test Case studies, but were not released until January, 1980, several months after the multiscanner data were processed by JPL to produce the images that we evaluated. The digital data processing was completed without recourse to that Kennecott support data, which included the only district-wide alteration maps of appropriate scale and detail. The timing of the release fortuitously provided us with a double-blind experiment wherein we attempted to recreate from remote-sensing data unseen maps produced by conventional techniques.

Published information includes a small-scale (1:150,000) geologic map of the Safford (Lone Star) district by P. C. Dunn (1978). Geologic cross sections in the literature are: Safford deposit by Robinson and Cook (1966), the Dos Pobres deposit by Langton and Williams (1982), and other parts of the district

by P. C. Dunn (1978). Geochemical, mineralization, and geophysical maps of the Safford deposit are shown in Robinson and Cook (1966). A district geochemical map is shown in Horsnail (1978).

3. *Procedures for Interpretation and Comparison of Data.* Interpretation of the Safford data proceeded in four steps: 1. Visual comparison between images and support data, primarily through the use of overlays; 2. Ground checking, collection of samples at the site to substantiate any interpretive conclusions, and to determine the cause of any unusual features; 3. Laboratory spectral reflectance and x-ray diffraction analysis of the samples; and 4. Further visual comparisons and integration with laboratory and ground spectral data.

The boundaries of distinctive spectral features were traced onto mylar from the various images, and the individual areas were classified and labelled according to similar spectral characteristics. Maps with supporting geological data were then placed on top of the appropriate images and compared with the interpreted overlays by the quick-flip technique. We used direct superposition of mapped geology and alteration on the color image products and the different image products on each other. We could compare lithologic and alteration separations and deduce qualitative image spectral signatures by internally comparing the image data suites themselves and externally comparing these with theoretical and measured spectra, x-ray diffraction results, field identification, and the support maps.

IMAGE PROCESSING

The following section on image processing was extracted verbatim from the excellent NASA report by Podwysocki, Gunther, and Blodget (1977).

"1. *Contrast Enhancements.* One of the more elementary processing techniques involves a contrast stretch of the raw digital information. Usually, the raw data received from a digital sensor system occupy a relatively small portion of the designed range for the system. These raw values can be stretched or expanded over the total dynamic range of a film processor by a digital scaling of the untreated data (figure 22). The resultant image contains information occupying the total range of film densities so that originally low-contrast images are made more contrasting. Various types of contrast stretches are available, requiring some judgement so that the most useful image is produced (Elston, 1976). Contrast enhancements of individual scanner channels may be combined to produce an enhanced color composite.

"Contrast enhancement of the raw multispectral data is advantageous for general interpretation but may not make use of all possible information that exists within a scene. Because it is only possible to combine any three bands with the primary colors to produce a color composite image, some information that may be crucial is lost and other information that may be redundant is included.

"Contrast enhancements may be applied to the raw data and almost invariably must be applied to data processed by the following procedures in order to make an interpretable image.

"2. *Banding Ratioing.* Banding ratioing has been shown to be a useful tool for mapping geological units (Rowan et al., 1974). A ratio can be thought of as a method for enhancing minor differences between two bands (see figures 20 and 21). In addition, differences in illumination due to topographic slope changes are minimized.

"Band ratioing also can be used as a method for dimensionality reduction. Up to six spectral bands may be combined into three ratios. Although not all rock types may be enhanced in any given combination, it is a useful product for reconnaissance, especially if there is a specific reason for the ratio choices (Rowan et al., 1974; Blodget et al., 1975). The resultant ratio image may be used to define training areas required for more rigorous enhancement procedures.

"If the band ratioing process is used as a general technique in an attempt to discriminate all possible lithologic units, the number of ratios is given by the formula: $N(N - 1)$, where N = number of channels. This amounts to 12 ratios for the Landsat satellite MSS, or six if their inverse permutations are disregarded. The possible unique ways that a given number of bands can be combined in groups of three for color composites is given in the formula: $\frac{[N(N - 1)]!}{3! [N(N - 1) - 3]!}$ where N = number of channels. Using the four Landsat bands as an example, this produces 20 possible ratio combinations without the use of inverse permutations, or 220 if they are included. Because the human eye can discriminate some color combinations more readily than others, each ratio composite should be investigated in several color combinations. $M!$ color combinations are possible, where $M = 3$, the three primary colors. Therefore, the previously mentioned ratio combinations could be increased six-fold if all possible color combinations were applied. It is obvious that this information-extraction process quickly becomes unmanageable and inefficient. In addition, many of the combinations are probably redundant.

"3. *Principal Components Analysis.* Principal components analysis has been utilized in statistical

processing of data for a considerable time and is well illustrated in numerous texts. Variations of this technique have been applied to image processing. The method produces new variables (components), which are linear combinations of the original variables; each component contains uncorrelated information. The process is useful because it utilizes all the data, requires no prior information and often reduces the dimensionality of the data so that the information may be displayed as an image in a color composite form. However, areas with bad data (dropout lines, bit slips), clouds, bodies of water, etc. may be excluded to force emphasis on the land surface.

"In a geometric sense, principal component analysis fits a new set of coordinate axes to the data, choosing as the first new axis or component an orientation that will maximize the variance accounted for by that axis (figure 23). A practical example using data from a portion of a Landsat image of Utah shows the variance-covariance matrix (Table 2), the eigenvalues (Table 3), and the transformation matrix (Table 4).

TABLE 2. Variance-Covariance Matrix for a Portion of a Landsat Image

MSS	4	5	6	7
4	125.50			
5	153.8	222.90		
6	122.3	183.9	165.60	
7	46.96	73.19	68.87	31.34

Variance-Covariance Matrix for the Waterpocket Fold scene (1014-17370). Values along the main diagonal of the matrix (trace) contain the variances for each MSS channel. MSS 5 has the greatest variability, followed by MSS 6, MSS 4, and least of all MSS 7. Values off the trace are the covariances; their non-zero values indicate an inter-relationship of bands. The total scene variance is given by the sum of the values along the trace.

"Based on the results of the two illustrated scenes and others that have been processed, the following generalizations can be made. Principal component analysis is a useful technique for discriminating rock and soil types if little prior information is available. All bands are processed rather than selected channels as in straight contrast enhancement or band ratioing. The data are dimensionally

TABLE 3. Eigenvalue Matrix after Principal Components Transformation for the Matrix in Table 3

Component	1	2	3	4
1	512.48			
2	0.0	25.20		
3	0.0	0.0	6.23	
4	0.0	0.0	0.0	1.43
% Variance Accounted for by Each Component	93.98	4.62	1.14	0.26

Values along the matrix trace are arranged in descending order. Total scene variance remains the same as in Table 3. The majority of the variance (93.98%) is now located in the first component with successively less in the higher numbered components. Off-trace values are now zero, indicating no inter-relation between the components. The percent variance accounted for by each component is determined by the component variance divided by the total variance.

TABLE 4. Eigenvector Matrix after Principal Components Transformation Based on Data of Tables 3 and 4

MSS Band Component	4	5	6	7
1	0.463	0.654	0.555	0.224
2	-0.760	-0.038	0.525	0.382
3	0.457	-0.728	0.315	0.404
4	0.002	0.202	-0.564	0.800

Component one has positive loadings (contributions) on all four MSS bands, with the first three being more important. The second component consists of negative loadings on MSS 4 and MSS 5 and positive loadings on the remainder; the loading of MSS 5 is insignificant. The negative loadings for component two can be interpreted as the contrast of MSS 4 and MSS 5 to MSS 6 and MSS 7.

reduced so that the resulting information often can be displayed in a three-color composite image. Information redundancy will be at a minimum. Success of the process will be somewhat dependent upon scene content, just as in the previously mentioned procedures. This is most evident in the higher order components, which may or may not incorporate usable information. Unlike contrast enhancement or band ratioing, ascribing a phenomenological attribute to an individual target is more difficult because the loadings that went into the production of a given component usually are based on the total scene content and not individual lithologic types.

"4. *Canonical Analysis.* Canonical analysis produces a data transformation based on spectral signatures of a set of targets (Seale, 1974; Merembeck et al., 1977). Mathematically, the process creates a set of transformed variables based on maximizing the among-category and minimizing the within-category covariance matrix. Geometrically, a set of mutually orthogonal, and hence uncorrelated, axes are fitted to the data by a rotation, translation and scaling, such that the first new variable or axis accounts for the greatest amount of variance with succeeding axes containing lesser and lesser amounts (see figures 24, 25, and 26).

"Canonical analysis is useful for dimensionality reduction and discrimination between rock materials where the differences may be small. It produces results similar to those of principal components analysis but is more time consuming because of the necessity for defining training categories. The process is most practical when other techniques do not produce satisfactory results. However, no amount of data processing or manipulation may be able to discriminate rock units which, although different to the geologist because of age, fossil content, composition, etc., exhibit the same spectral characteristics for any given sensor system.

"Band ratio images often achieve better separation of some rock types and allow for some data compression; however, for a thorough analysis the number of possible ratio combinations to be investigated makes the process expensive and time consuming. Principal component and canonical analyses are advantageous because of the inherent data compression capabilities of either process. The former technique is an inexpensive first approach to rock discrimination and produces results quite similar to the latter method but has a higher dependence upon general scene content. Of these two methods, canonical analysis excels when the differences between rock types are small because the transformation depends upon the target areas chosen."

THE KENNECOTT DEPOSIT

This section describing the Kennecott deposit is taken from Robinson and Cook (1966).

1. *Lithology.* The Mesozoic host rocks that contain the Kennecott ore body consist of Cretaceous to early-Tertiary andesite and dacite volcanic rocks intruded by quartz diorite, granodiorite, and quartz monzonite porphyry stocks, and rhyolite, latite, quartz latite, and related dikes (figures 5 and 6). Lithic tuff and grit fill a volcanic vent shown near the center of figure 5 (as Ta). The Lone Star stock, the parent pluton, occupies a large part of the northwest quadrant of this figure. Postmineral basalt (Ta) and more acidic (Ta) mid-to-late Tertiary volcanics cover the Kennecott ore body.

2. *Mineralization.* The orebody consists of the primary minerals pyrite and chalcopyrite with lesser amounts of bornite and chalcocite. Pyrite is the most abundant sulfide present. The pyrite halo is exposed at the center of the map (figures 7 and 8). Secondary minerals include chalcocite and covellite.

Chrysocolla is the most abundant oxide mineral present. Goethite and hematite have replaced sulfide and primary iron-bearing minerals. Transported limonite has filled fractures and coated the rocks yellow to brown.

3. *Structure.* The Kennecott deposit is localized in an extensive sheared zone thousands of feet wide termed the "Lone Star shear zone" (figures 9 and 10). The Lone Star shear zone occupies the 6,000-foot-wide corridor between the Lone Star and At Ease faults that extends at least 5,000 feet under the Tertiary volcanics. Displacement along the shear zone could be as much as 800 feet. The Trojan fault is a normal fault that displaces the Tertiary younger volcanics, with 170 feet dropped on the southeast side.

4. *Alteration.* Figures 14 and 15 show alteration zones as mapped in the field approximately 20 years ago. The following section on alteration is quoted from Robinson and Cook (1966).

"...an area 12,000 by 6,000 feet was subject to extensive hydrothermal alteration. Half of this area is exposed, and the balance is covered by the later Tertiary volcanics...

"A central area of intense alteration is composed of a strongly developed quartz sericite zone on the southwest, which adjoins and is partially superimposed on a large area of pervasive secondary biotitization on the northeast. The ore body is in these two zones around which are arranged the chloritic and propylitic zones in a roughly concentric pattern. Part of the quartz sericite and the chloritized zones is in essentially pyritized areas. The propylitic zone is, however, unmineralized except where traversed by shear

zones, veins, or dikes that may be accompanied by sulfides--pyrite and (or) chalcopyrite. Alteration boundaries are rather arbitrary in that mineralogical changes are transitional and overlapping, particularly in the porphyritic andesite host rock. The influence of rock type and structure is also important because the quartz sericite zone corresponds mainly with the post-andesite intrusive complex and also with the pyroclastic lithic tuff and volcanic vent debris. Sericitic alteration not only occurs in all dikes but also along their contact zones with the porphyritic andesite--in both the chloritic and propylitic zones--as much as 10,000 feet southwest of the ore body. Sericitization is clearly later than biotitization in gross field pattern, wherein the biotitized rock contains sheaves of sericitized rock along veins, shears, and contacts. Microscopically, it is clear that biotite is also altered to sericite along these zones.

"In most of the intrusives potash feldspar, probably primary, makes up 15 to 20 percent of the groundmass. In some instances, however, there is a concentration of potash feldspar along veins, indicating either addition to the rock or possible segregation of primary potash feldspar during alteration. In the andesite, secondary potash feldspar and associated quartz and sericite are abundant along veins.

"Prior to the development of sericite, the plagioclase in the andesite--andesine--had been altered largely to oligoclase or albite. In the intrusives, albitization had also taken place at an early stage.

"QUARTZ SERICITE ZONE. Rocks that have undergone this type of alteration--occurring mainly over an area of 7,000 by 5,000 feet--are characteristically bleached to a white or light-gray color. This alteration stage appears to have been later than the other stages. The rocks of acidic to intermediate composition composing the dikes, plugs, and volcanic vent debris were the most severely affected. Both plagioclase phenocrysts and plagioclase in the groundmass were thoroughly converted to sericite and quartz--largely along veinlets. Mafic minerals were similarly affected. The biotitized andesite, where adjacent to faults, intrusive contacts, veins, and shears, was also altered by conversion of mafics and plagioclase to sericite, quartz, and minor sphene. Those zones are relatively narrow and exhibit gradational boundaries from pervasive sericitic content into the biotitized andesite. The superimposition of the quartz sericite zone on the biotitized zone is, thus, clearly demonstrated. A similar relation of this type of alteration to the chloritic and propylitic zones is also apparent...

"It is of interest to note that the potassium-argon age dating of the sericite is 53 m.y. or slightly

younger than the San Juan and Lone Star stocks.

"BIOTITE ZONE. The rocks mainly affected by this type of alteration are the porphyritic andesites. Hornblende and augite were replaced by brown biotite in flakes, clots, and, more rarely, in veinlets carrying sulfides. The strongest biotitization--10 to 50 percent and averaging about 20 percent--is developed around the intrusive plugs and dikes in and adjoining the ore body. The acidic to intermediate intrusive rocks have secondary biotite developed in only minor amounts, a few percent, along quartz veinlets. Other occurrences in these intrusives, if ever present, were probably destroyed by the later sericitic alteration phase...

"CHLORITE ZONE. Chlorite is the most widely distributed alteration mineral and occurs in all stages of alteration. However, as shown on the map, a predominantly chloritic zone 1,000 to 2,000 feet wide surrounds and overlaps the biotitized and sericitized zones on the southwest of the ore body... The boundaries of the chloritic zone are arbitrarily drawn when mafics are more predominantly replaced by chlorite than by secondary biotite.

"PROPYLITIC ZONE. This is the most widespread zone and represents the area of lowest alteration intensity. Epidote and to a lesser extent chlorite are the common secondary minerals. The relation of this zone to mineralization and other alteration processes is not clear, but it appears to have been very early and possibly deuteritic in origin.

"SUPERGENE ALTERATION. As already mentioned, alteration of the outcrop and sub-Tertiary volcanic outcrop has produced a typically conspicuous colored cap rock over the ore body and over the mineralized veins and shear zones. The color of the rock is related in intensity directly to the amount of former sulfide content and to the degree of oxidation and weathering to which it has been subjected.

"The dikes and plugs that have undergone sericitic hydrothermal alteration are inherently bleached. Weathering of the sulfides has also produced oxidized compounds, which have stained these light-colored rocks various hues of yellow, brown, red, maroon, and black. The biotitized and chloritized porphyritic andesites tend to be relatively darker in color, although oxidation of the iron compounds together with leaching have actually produced a lighter colored rock in the zone of weathering. This grades into dark-gray, black, or green rock in the primary zone below. Although some of the micaceous minerals in the weathered biotite zone may actually be sericite, it is thought that most of this material is biotite from

which the iron has been leached by weathering.

"The minerals that create the conspicuous color in the leached rock over the ore body are predominantly the ferric iron compounds goethite and hematite. Jarosite and alunite are more abundant over the pyritic halo.

"Kaolin, alunite, and montmorillonite are developed to the greatest extent along larger shears, faults, and selvages on contacts where movement has occurred. Apparently the sheared, fractured, and crushed rock was extensively converted to kaolin along the channels followed by acid-charged ground water. Beyond these channels kaolin is developed to only a minor degree...."

5. *The NS-001 Canonical Transform Image and Its Interpretation.* Figure 12 is a photographic copy of a small portion of a digital image generated at the Jet Propulsion Laboratory from magnetic tape data acquired by NASA's airborne NS-001 multispectral scanner survey of the Safford district. The scanner recorded ground radiance in eight bands that included the seven Landsat-D Thematic Mapper bands located in the spectrum at:

<u>Band</u>	<u>Center Wavelength in Microns</u>
1	.48 greenish blue
2	.56 yellow green
3	.66 red
4	.83 reflective infrared
5	1.6 reflective infrared
6	2.2 reflective infrared
7	11.0 thermal infrared

The thermal band number 7 was not included in the canonical transform processing of the remaining (reflective) bands. The red, green, and blue colors that were composited in figure 12 were arbitrarily assigned to represent the 2nd, 3rd, and 1st principal components, listed in order of their importance. Information from all six bands is represented in each of the components in different proportions.

The spectral anomalies (or spectral clusters) that represent phyllic alteration are shown as red or yellow in figure 12 and are outlined in the figure 13 cartoon. The numbered points on figure 13 indicate the locations of the samples taken for laboratory reflectance spectra (figure 25) and x-ray diffraction analysis. The yellow-coded areas seem to represent quartz sericite alteration, whereas the red-coded areas include chloritization with local biotite and quartz sericite. Much of the propylitic zone is shown as steel blue in the canonical transform.

THE DOS POBRES DEPOSIT

The following geologic description and figure 17 of the Dos Pobres area are quoted from Langton and Williams, 1982.

1. *Lithology.* "SAFFORD METAVOLCANICS. More than 75 percent of the ore at Dos Pobres occurs in the Safford metavolcanics, a metamorphosed Cretaceous-Tertiary sequence. The bulk of the volcanic pile is andesitic in composition, but dacites, dacite tuffs, and latites have been recognized. Specifically, the majority of the flows and breccias are hornblende or pyroxene andesites that have been pervasively altered in the vicinity of the orebody. The fragmental nature of the flow breccias is often obscured by metamorphism or hydrothermal alteration, but it may be accentuated by crackling. Contact metamorphism by the parental granodiorite has been clearly dated at 69.8 ± 2.7 m.y.

"PRODUCTIVE PORPHYRIES. Some of the higher grade copper values occur in the dikes or phacoliths in the upper levels of the mine, but with depth the porphyries become progressively lower grade and relatively barren...

"...the principal productive porphyry is generally a quartz monzonite, ranging in composition to tonalite or granodiorite...

"HORNBLLENDE ANDESITE DIKES AND SILLS. Intrusions in the form of hornblende andesite dikes and sills are most obvious in the east-northeast-west-southwest shear zones away from the ore, and most of them are clearly consanguineous with the Baboon volcanics. Large titaniferous hornblende phenocrysts, often more than 1 cm long, suggest that these nonproductive intrusions were saturated with water. The dikes, which are evidently late- and post-mineral, acted as dilutents to the ore. Ore grade in their vicinity is invariably lower than in the core of the orebody, where no dikes or sills have been recognized. These intrusions are generally only a few feet thick in the Safford metavolcanics, but they may reach thicknesses of more than 200 ft. in the lower Baboon sequence.

"BABOON METAVOLCANICS. The propylitized andesitic agglomerates, flow breccias, mud flows, and lithic tuffs of the Baboon metavolcanics crop out northeast, north, and northwest of the orebody and thicken to more than 1,500 ft. northwesterly. The sequence has been hydrothermally altered locally, but has not been metamorphosed by either the productive porphyries or the parental pluton(s). Propylitization appears to

be autometamorphic away from the east-northeast-west-southwest shear zones, but is clearly hydrothermal toward the orebody. Lower members of these volcanics are intruded by the aforementioned hornblende andesite dikes of late- or post-mineral age, and the upper units contain large xenoliths of the same intrusions, with coronas that indicate the dike fragments were cooling with the flows."

2. *Structure.* "Two of the most important structures that influence the geometry of the orebody are the Foothill fault and the Dos Pobres anticline (see figure 17). It was initially thought that folding resulted from older lateral movement along the Foothill fault, but more recent evidence clearly suggests that the drag fold is a secondary feature related to the Valley and Red Dyke faults. A northwest-southeast cross section parallel to the Foothill fault demonstrates fold control for the core....

"...Several east-northeast-west-southwest faults have had considerable post-mineral displacement, but these structures were the principal channels for productive porphyries and ore-bearing fluids. Essentially contemporaneous with the major down-throw of the Foothill fault, these veins had recurrent movement and down faulted the ore in a step-like pattern from southeast to northwest.

"Crackle brecciation constitutes the dominant fracturing in the mine and is most extensive in the metavolcanics, not in the productive porphyries. All of the crackling or fracturing not related to post-mineral faulting appears to be hydrothermal in origin. Simple parting across fragments and large phenocrysts, with virtually no displacement of the respective boundaries, is typical of the character of this fracturing and is seen throughout the orebody.

"Contact breccias intimately associated with the porphyries often host the highest grade ore; these features are more important in the upper portions of the deposit and must have formed early during intrusion. Typically, the upper extremities of dikes grade into the breccias, which are characterized by numerous fragments of metavolcanics embedded in the porphyry.

"A later event was the development of a megabreccia, which was apparently related to the de-gassing of the productive rest-magma. This breccia incorporates huge fragments of meta-andesite, productive porphyry, and contact breccia. The overall appearance of the megabreccia suggests 'floating' blocks of the porphyry in a crackle breccia....

"Arguments can be made for post-ore tilting and low-angle faulting in the Lone Star mining district,

especially at the Dos Pobres deposit. However, any significant tilting that did occur must necessarily have preceded the Miocene extrusive period, as these younger volcanics have an average dip of approximately 12° NE near the orebody. Until further information is obtained, it must be assumed that the Dos Pobres orebody has been tilted between 12° and 25° NE...

"Erosion appears to have been more extensive southeast of the Dos Pobres orebody. The Baboon volcanics are not present 4 miles southeast of the deposit, but they thicken to at least 1,500 ft. northwest of the orebody.

"Low-angle faulting has been recognized at the Dos Pobres orebody, but it is most difficult to trace the structures for any distance along strike. This faulting apparently preceded or was contemporaneous with the early stages of Miocene volcanism... .

"The Oligocene-Pliocene Gila Mountain Volcanics were extruded on an erosional surface that had exposed all of the Laramide intrusives and consanguineous metavolcanics. The source of these volcanics was to the northeast along Bonita Creek, and this arcuate volcanic chain may be mapped in the Peloncillo Mountains as far southeast as Stein's Pass, New Mexico. Contemporaneous with this volcanism, a pediment was forming along the southwest front of the Gila Mountains, and the gravels derived from it thicken rapidly toward the center of the Safford Valley.

"Basin and Range block faulting represented the last major tectonic event in the district. The northwest-southeast faults were particularly active, and gravity displacements in excess of 2,000 ft. have been recognized on several of the high-angle structures. Additional adjustments on north-south and northeast-southwest faults also occurred, but apparently they were not of the magnitude of those in the Foothill, Red Dyke, Valley and Butte faults. District tilting of at least 12° NE can be justified during these adjustments. Finally erosion and oxidation of the orebody and development of extensive thicknesses of clay beds, basin fill, terrace gravels, and alluvium during Pliocene and Recent periods established the environment as it now appears."

3. *Alteration.* "ALTERATION OF PORPHYRY. The productive porphyry at Dos Pobres is generally a quartz monzonite by mode; however, the freshest samples seen tend to be granodioritic, as attested by phenocrysts of embayed β quartz, plagioclase, hornblende, and dark brown biotite. The matrix carries β quartz,

plagioclase, hornblende, quartz, and orthoclase. It seems likely that the porphyry was indeed a granodiorite originally, and that it was modified locally and erratically by late magmatic effects.

"The productive porphyry is generally seen in the form of dikes or fragments of dikes in the center of the orebody. These dikes have been dated at 52.2 ± 2.0 m.y. A more coherent stock of the porphyry, which has been dated at 47.8 ± 1.8 m.y., occurs at depth in the northwest part of the deposit....

"...The earliest change to occur is the replacement of hornblende by biotite flakes, which appear identical in character to the biotite phenocrysts, but which may also crystallize as frilly rings or overgrowths on the larger books themselves. This alteration is surely of late magmatic age. Coarse primary biotite has been deformed by flowage, whereas this new biotite has not. It is probable that, when this biotite alteration was taking place, the wall rocks were undergoing mesozonal metamorphism.

"With continued cooling, late magmatic biotite ceased to form and a new assemblage began to crystallize; quartz + orthoclase + magnetite + bornite. Quartz and orthoclase grow in the matrix at the expense of plagioclase and late magmatic biotite. The orthoclase thus formed is clear and generally non-perthitic. At this stage the rock seems quite normal, and one might not suspect any alteration, but the mode is that of quartz monzonite. This metamorphosis probably began as late magmatic but continued into the deuteritic stage, for it is often fracture controlled as well as pervasive. Bornite is seen most often in fractures, with quartz and orthoclase; these veinlets have a distinctly hydrothermal aspect. This stage of alteration doubtless coincided with the main pulse of mineralization in the wall rocks and with the period of intense K-metasomatism seen in them.

"In most places this episode ended, as cooling continued, with simple deuteritic alteration. Any biotite surviving, usually with phenocrysts, was partially replaced by coarse clinocllore and blebs of epidote with accessory rutile; the chlorite may be accompanied by minute platelets of hematite. Plagioclase is altered mildly to shreddy sericite and some earthy epidote. Usually only the cores of phenocrysts are so afflicted, and sodic rims remain unchanged. Sulfides remained mobile in veins at this time, with chalcopyrite joining bornite in a gangue of quartz, carbonates, and chlorite....

"In some places, however, the porphyry shows incipient alteration to a quartz-sericity assemblage. This alteration is of deuteritic age and occurs in areas where more sulfur was available. While such alteration

is seldom complete, the tendency is for groundmass quartz to grow to the point of coalescing, while all remaining feldspars and altered mafites are partially replaced by sericite. Any chlorite that survives is highly magnesian, and even amesite may be present. Pyrite may appear and bornite yields to chalcopyrite. These sulfides occur in quartz veinlets or may be disseminated in sites of former mafites. Alteration of this nature is uncommon and seldom complete, as is typical of low-sulfur porphyry copper systems elsewhere. The best example of such alteration is locally observed on the southeast side of the orebody....

"... During the series of alteration steps from fresh to deuteric to new biotite, SiO_2 decreases, while Ti, Na, Al, and Fe increase; these changes are due in large measure to the appearance of abundant new biotite. The lack of important changes in K_2O reflects the loss of orthoclase during biotite crystallization and implies no real K-metasomatism within the intrusive....

"...The elements that show considerable change are those whose mobility is closely tied to the presence of sulfur. Calcium is the best example, for it is quickly removed when sulfur is available; elements such as Si and Al increase only because they are residual, and there is a corresponding decrease in the volume of the original rock. The assemblage quartz-sericite-rutile derives readily from plagioclase-sphene in the presence of sulfur, and the loss of Ca from plagioclase is inevitably the major change.

"ALTERATION OF WALL ROCKS. The history of events in the andesite pile that hosts the productive porphyries and most of the copper values has been somewhat more complex. The pile exhibits an epizonal metamorphic (alteration) event of almost regional extent that is believed to be the composite effect of two processes. One process was undoubtedly the slow cooling of such a thick, rapidly extruded pile that yielded an autometamorphism or 'stewing' in the epizone. We suggest a slowly cooling heat source below as the second cause for the abnormally strong epizonal effects in the volcanic rocks of the district, which are in contrast to those effects in many other thick piles of mafic volcanics. This source of heat must have been the granodiorite or parent pluton of batholithic dimensions (the Lone Star pluton) underlying the district.

"As a result of prolonged cooling, the andesites demonstrate an alteration characterized by stability of epidote and pennine. Both minerals may replace mafic minerals completely as coarse-grained epidote prisms embedded in pennine. Epidote singularly replaces plagioclase in part, and the surviving plagioclase is albitic in nature. Excess iron, derived from mafic minerals and accessory magnetite, appears as tiny

hematite tablets *in situ*. Although calcite is not abundant, its presence in the volcanics is commonplace, and it may form patchy crystalloblasts in the matrix. In contrast to the dominant andesites in the pile, dacites responded somewhat differently; they were altered to an assemblage of quartz-sericite-pennine with epidote rare or absent.

"The second alteration event, imposed on the volcanics in the aureole around the Dos Pobres deposit, was identical to the first and was due to rising temperatures that resulted from intrusion of the productive magma. Again epidote and pennine formed, often merely as continued development of the same earlier formed minerals, but with exaggerated growth. Plagioclase may be totally destroyed, and clots or pods of coarse epidote, with interstitial calcite and pennine, spread crystalloblastically and invade the surrounding matrix. It has been observed that any nucleus might have initiated this process, such as a large plagioclase phenocryst or perhaps an especially reactive xenolith or merely a fracture intersection. Some clots do show epidote veinlets leading away in one or two directions. This early zone dies out away from the productive porphyry and merges insensibly into the more regional propylitization of identical mineralogy. Effects cannot be seen with any certainty beyond about 2,000 ft. from the periphery of the orebody.

"With continued rising in temperature and final emplacement of the productive magma, mesozonal metamorphism began. The earlier assemblage vanishes and the andesites exhibit abundant secondary actinolitic hornblende and brown biotite, which has been dated at 56.9 ± 2.2 m.y. Both minerals occur as small crystals that vigorously attack both relict plagioclase and hornblende. The new actinolitic hornblende is not Fe rich, and disseminated dust-like magnetite is a common accessory in this assemblage. In many samples the disseminated magnetite is concentrated in hazily defined areas suggestive of the outlines of former cognate xenoliths.

"Early mesozonal metamorphism was merely a transient stage, for as more K_2O was added during mesozonal conditions, the assemblage yielded to a metasomatic one.... This alteration represents the main pulse of K-metasomatism and mineralization, and, where most intense, it may affect even the productive porphyry dikes. As an end result, these dikes may be so heavily replaced by secondary biotite that they are indistinguishable from the andesites, except for the ghost of biotite phenocrysts....

"Crackling appears to have been an important mechanism during the mesozonal K-metasomatism, while it

was relatively unimportant during the preceding mesozonal metamorphism. The wall rocks were laced with fractures that are now veinlets carrying quartz, orthoclase, apatite, bornite, and chalcopyrite...

"The biotite zone may be seen up to 1,600 ft. from the center of the orebody; then it gradually fades and merges into the surrounding propylitic assemblage. Toward the outer parts of the zone biotite becomes notably paler and assumes a green color. The effect is first shown by biotite formed at the expense of plagioclase, whilst biotite developed in the matrix is still brown; but eventually this, too, assumes a green color....

"Subsequent to (post-ore) tilting, oxidation and erosion were the dominant forces at work during Oligocene and early Miocene times. Also at this time minor supergene enrichment was superimposed on the hypogene ore in the Dos Pobres deposit. The central portion of the Dos Pobres chalcopyrite-bornite ore pipe was partially leached, thoroughly oxidized, and locally enriched to depths of approximately 1,200 ft. (2,900 ft. level). Sulfides in the periphery of the marginal zone and in the pyritic aureole, however, are often within 300 ft. of the surface on the southeast side of the orebody. Chrysocolla and cuprite are the dominant copper oxides for depths of 1,000 ft. over the center of the sulfide ore, but subordinate amounts of tenorite and brochantite have been recognized. Native copper, chalcocite, and covellite are abundant in the mixed oxide-sulfide zone between the 2,900- and 3,300-ft. elevations. Oxide ore averages 0.62 percent Cu, compared to 0.72 percent for the sulfide ores. Hematite, jarosite, and limonite capping on the southeast side of the orebody also reflects minor chalcocite enrichment in the vicinity of the productive porphyries."

4. *The NS-001 3-Ratio Image and Its Interpretation.* Figure 18 is an enlarged portion of the digital image produced by the Jet Propulsion Laboratory from the same NS-001 airborne scanner tape that produced the image shown in figure 12. However, the image in figure 18 was made by a band-ratioing technique to produce a 3-ratio false color composite using the following codes:

1.6/2.2	red	=	high values;	cyan	=	low values
.66/.56	green	=	high values;	magenta	=	low values
.83/1.1	blue	=	high values;	yellow	=	low values

The numbers represent the center wavelength of the bands whose intensities were ratioed pixel-by-pixel.

According to published laboratory spectral measurements (Hunt and Ashley, 1979), ground areas whose surface has a high percentage of clay minerals associated with phyllic alteration and argillization would have a high 1.6/2.2 ratio and thus would be colored red on the image. Areas high in ferric iron would have a high .66/.56 ratio (high red-to-green ratio) and would be coded green. A combination of high ferric iron and high "clays" would produce a yellow code. Figure 19 is a cartoon showing the sites of conspicuous yellow-to-red-coded spectral anomalies and the location of samples taken for laboratory spectral reflectance and x-ray diffraction analyses. The magenta patterns in the arroyos represent verdent vegetation (compare the areal photograph of figure 16 to the ratio image of figure 18).

The red-to-orange area that included sample F (figure 19) should, according to our spectral model, contain large amounts of clay. Our field inspection of that site showed that it is a highly argillized productive porphyry (see figure 17, geologic map). Analysis of samples showed major alunite. Sample numbers C, D, and E all contained kaolin. Sample B on the other hand contains major chlorite and minor calcite. One might conclude then that figure 19 is a map showing the boundaries of phyllic alteration and that figure 18, the 3-ratio image, has demonstrated that the NS-001 multispectral scanner was operating as an airborne alteration mapper. The participants of this field trip are invited to test this hypothesis.

REFLECTANCE SPECTRA AS DIAGNOSTIC DATA

Our examination of the computer-generated 3-ratio and canonical transform images of the Safford district (of which figures 12 and 18 are but small samples) indicates that these remotely sensed images could have been used to produce an alteration map very similar to the alteration map produced by field mapping. Figure 14 is a small section of an alteration map released by Kennecott Corp. after the NS-001 images were produced. Taking these 1:24,000 scale alteration maps into the field with the 3-ratio and canonical scanner images and color aerial photography, we confirmed by field investigation that the scanner images could indeed have directed us to phyllic alteration haloes.

We wanted next to determine the extent to which the spectral signatures of rocks, as mapped by the Thematic Mapper, can be used in mineralogical remote sensing. We collected the surface rock samples marked on figures 13 and 19 at sites of distinctively coded spectral environments shown on the scanner

images as distinctively coded false (arbitrary) colors. These samples were then subjected to x-ray diffraction analysis and to reflectance spectrometry at Jet Propulsion Laboratory (by K. Baird) and to reflectance spectrometry at the University of Arizona, Optical Science Center (by E. Shih).

The integrating sphere reflectance spectrometer at the Optical Science Center has a sample chamber large enough to hold a hand-size rock sample and obtain reflectance spectra of various surfaces of the rock. We measured the continuous reflectance spectra from 0.4 to 2.7 microns of both fresh, broken surfaces and the unbroken, weathered rind of all samples. The resulting spectra for those samples that fall within the maps of this Field Guide are shown in figures 25 and 26.

1. *Dos Pobres Spectra.* The spectral line profiles labeled G, A, B, E, E_d, and F on figure 25 and at the bottom of figure 26 represent samples collected at these points shown in figure 19. The spectra on the left describe the visible and infrared "colors" of the weathered rinds and the spectra on the right describe the "colors" of the fresh, broken surfaces of these same rock samples. Note that they are different. For example, compare profile B on the left with profile B on the right.

These diagrams are labeled to show the spectral positions of the six solar bands of the Thematic Mapper. Three bands fall within the visible range at .48 (blue-green), .57 (yellow-green), and .66 (red) microns, and three are in the solar (non-thermal) infrared range at .83, 1.6, and 2.2 microns. It can be seen from the spectra that the ratio of reflectance at 1.6 microns to reflectance at 2.2 microns alone would be sufficient to discriminate between the samples taken from the argillized productive porphyries (E, E_d, and F) and those taken from the propylitically altered areas (G, A, and B) of the Dos Pobres deposit. Samples E and F contain major kaolin and major alunite, respectively. The steep 1.6/2.2 slope is indicative of these two "clay" minerals. The notch at .90 microns and the steep .57/.66 negative slope is typical of hematite.

2. *Kennecott Spectra.* The spectral profiles at the top of figure 26 are from the weathered and fresh surfaces of rock samples taken from the Kennecott alteration halo at points marked on the map of figure 13. Note that the spectra of the weathered rinds (left) are more distinctive than those of the fresh surfaces (right). In the Safford environment the weathering effects have enhanced the diagnostic character of the spectra, especially in the non-visible (greater than .7 microns) parts of the spectra. This weathering

enhancement of infrared spectral features is fortunate because remote sensors usually view the undisturbed, weathered rock surfaces.

Sample 2g contains kaolin, sericite, and chrysocolla. Note the green hump at .57 microns. Sample 2d is dark from the presence of chlorite, but also contains montmorillonite. Sample 1 contains hematite (note the deep .90 notch), sericite, and illite (steep 1.6/2.2 slope). Sample 3 was taken from the rhyolite lithic tuff (note the high visible reflectance of the fresh surface) that contains sericite and kaolin and a trace of hematite.

The spectra above suggest the following conclusions.

1. Some mineral classes can be separated by their spectra, namely iron oxides and the "clay" minerals, thus making possible the discrimination between propylitic and phyllic alteration zones.
2. The infrared portion of the spectrum is more important than the visible spectrum for mineral identification.
3. The weathered rind of exposed rock surfaces has spectra different from the broken surface, especially in the infrared.

TABLE 1. Geologic Column and Geochronology of the Safford District (after Langton and Williams, 1982)

Name	Rock Type	Thickness	Age	Events	Dates (m.y.)
Alluvium, terrace gravels, basin fill	Sands, clay beds, gravels, siltstones, conglomerates	0-2,000'+	Pleistocene-Recent	Younger pediment, basin fill, and gravel development	-
-----UNCONFORMITY-----					
Gila Mountain volcanics	Basalt & rhyolite dikes, sills, plugs. Basalt flows, tuffs, rhyolites, agglomerates, vent debris, basal conglomerate	0-3,000'+	Miocene-Pliocene	Basaltic volcanism Major Basin and Range gravity faulting, minor tilting, erosion, and oxidation Intrusion - Extrusion of Gila Mountain volcanics contemp. with development of older pediment	- - -
-----UNCONFORMITY-----					
	Hornblende andesite dikes, sills, plugs	-	Eocene	Extrusion of upper Baboon agglomerates Late, prolific retrograde veining	46± - 36± 46±
Baboon metavolcanics-metavolcaniclastics	Propylitized andesite agglomerates, flow breccias, mud flows, lithic tuffs, conglomerates	0-1,500'+	Eocene	Extrusion of lower Baboon volcanics and pyroclastics Intrusion of hornblende andesite magma(s) Degassing and subsequent crystallization of productive rest magma(s) with accompanying hydrothermal phase	47± - 46± 47± - 36± 47.8 ± 1.8
-----UNCONFORMITY-----					
Productive Porphyries	Tonalite-quartz monzonite-monzonite-granodiorite porphyry stock(s), dikes and sills	-	Paleocene-Eocene	Uplift, faulting, minor folding, continued volcanism Crystallization of productive porphyry dikes Early pervasive mesozonal contact metamorphism and hydrothermal alteration Intrusion of productive magma(s)	52.2 ± 2.0 56.9 ± 2.2 59± - 47±
Lone Star Pluton(s)	Quartz diorite-granodiorite batholith	-	Upper Cretaceous-Paleocene	Uplift, faulting, NE folding, erosion, deposition of volcaniclastic sediments	-
Safford metavolcanics-metavolcaniclastics	Metamorphosed hornblende and pyroxene andesite flows, breccias, agglomerates, wackes, and mud flows	3,500'+	Upper Cretaceous-Paleocene	Crystallization of Lone Star pluton(s) Intrusion of Lone Star magma(s) into Safford volcanics and subsequent contact metamorph. Extrusion of Safford volcanics Intrusion of Lone Star magma(s) into Precambrian metasediments and subsequent contact metamorphism	67± - 60± 69± - 60± 70± - 60± 69.8 ± 2.7
-----UNCONFORMITY-----					
	Amphibolite, gneiss, granite, quartzite, schist	-	Precambrian	Uplift, faulting, erosion	

REFERENCES

- Abrams, M., Brown, D., Lepley, L.K., and Sadowski, R., 1982, Landsat-D TM application to porphyry copper exploration. Proc. 2nd IEEE Internat. Geol. and Remote Sensing Symp. (GARSS), Munich, Germany, June 1982 (in press).
- Blodget, H.W., Brown, G.F., and Moik, J.G., 1975, Geological mapping in northwestern Saudi Arabia using Landsat multispectral techniques. NASA Earth Resources Surv. Symp., Houston, TX., July 1975, TMX-58618, p. 971-989.
- Elston, D.P., 1976, Geologic evaluation of north-central Arizona. U.S. Geological Survey Prof. Paper 929, p. 59-60.
- Dunn, P.G., 1978, Regional structure of the Safford district, Arizona. Ariz. Geol. Soc. Digest XI, p. 9-15.
- Horsnail, R., 1978, Geochemistry of the Safford district, Graham County, Arizona. J. Geochem. Explor., v. 9, p. 241-243.
- Hunt, G. R., and Ashley, R.P., 1979, Spectra of altered rocks in the visible and near infrared. Econ. Geol., v. 74, p. 1613-1629.
- Langton, J.M., and Williams, S.A., 1982, Structural, petrological, and mineralogical controls for the Dos Pobres orebody: Lone Star mining district, Graham County, Arizona, in Titley, S.R., ed., Advances in geology of the porphyry copper deposits, southwestern North America. Tucson, Univ. Arizona Press, p. 335-352.
- Merembeck, B.F., Borden, F.Y., Podwysocki, M.H., and Applegate, D.N., 1977, Application of canonical analysis to multispectral scanner data. Proc. 14th Annual Symp. of Computer Applications in the Mineral Industries, Univ. Park, Pa., Sept., 1976.
- Podwysocki, M.H., Gunther, F.J., and Blodget, H.W., 1977, Discrimination of rock and soil types by digital analysis of Landsat data. NASA X-923-77-17.
- Rehrig, W.A., and Heidrick, T.L., 1972, Regional fracturing in Laramide stocks of Arizona and its relationship to porphyry copper mineralization. Econ. Geol., v. 67, p. 198-213.
- Robinson, R.F., and Cook, Annan, 1966, The Safford copper district, Lone Star mining district, Graham County, Arizona, in Titley, S.R., and Hicks, C.L., eds., Geology of the porphyry copper deposits, southwestern North America. Tucson, Univ. Arizona Press, p. 251-266.

Rowan, L. C. et al., 1974, Discrimination of rock types and altered areas in Nevada by the use of ERTS images. U. S. Geological Survey Prof. Paper 883, 35 p.

Seale, H.L., 1964, Multivariate statistical analysis for biologists. Methnen & Co., London, 209 p.

RECOMMENDED READING

Siegal, B.S., and Gillespie, A.R., 1981, Remote sensing in geology. Wiley, 702 p.

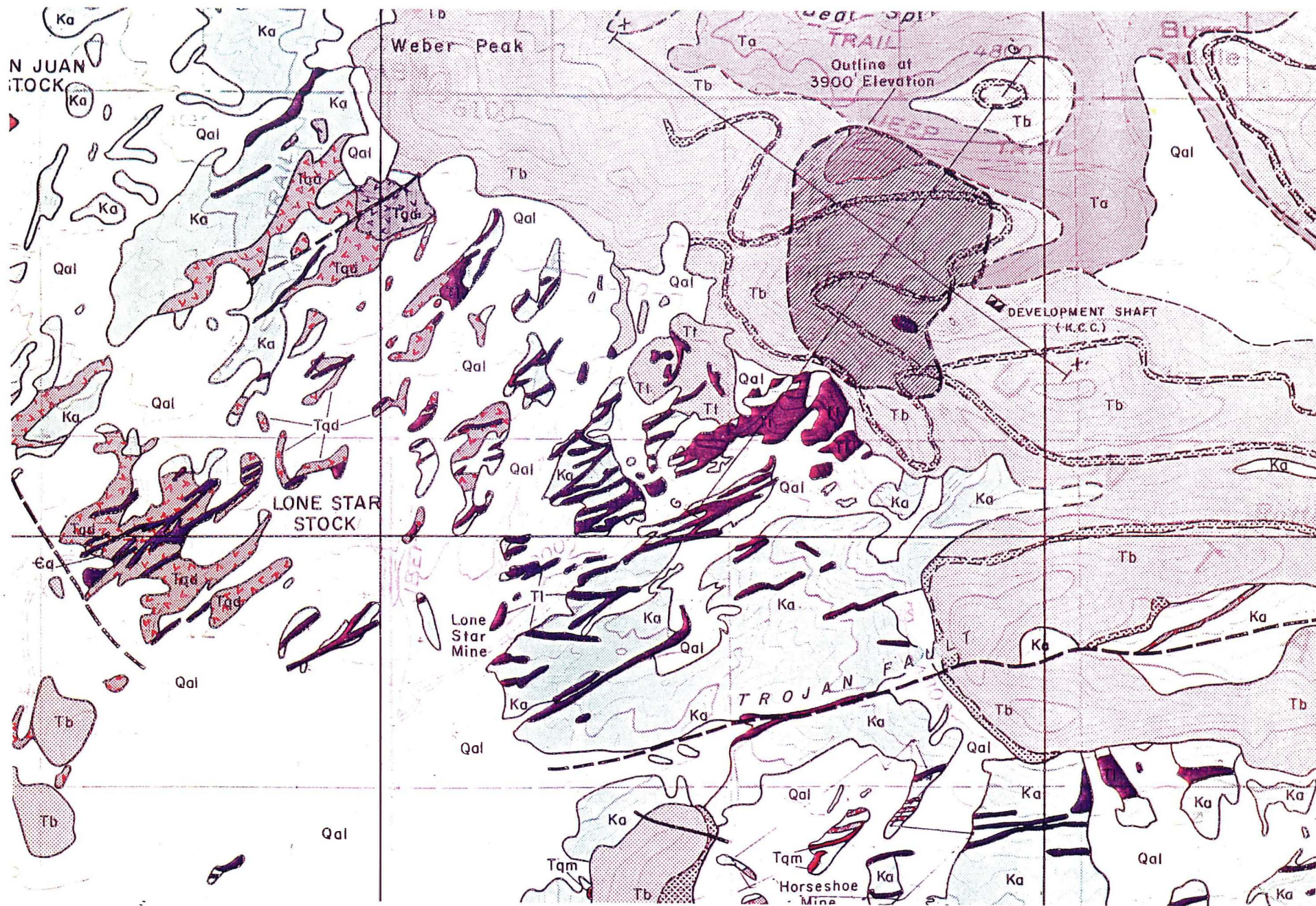


Figure 5. Geologic map, vicinity of Kennecott deposit, 1:24,000 scale (courtesy of Bear Creek Mining Co., Kennecott Corp.).



Figure 7. Map of mineralization distribution, vicinity of Kennecott deposit (courtesy of the Kennecott Corp.).

LEGEND

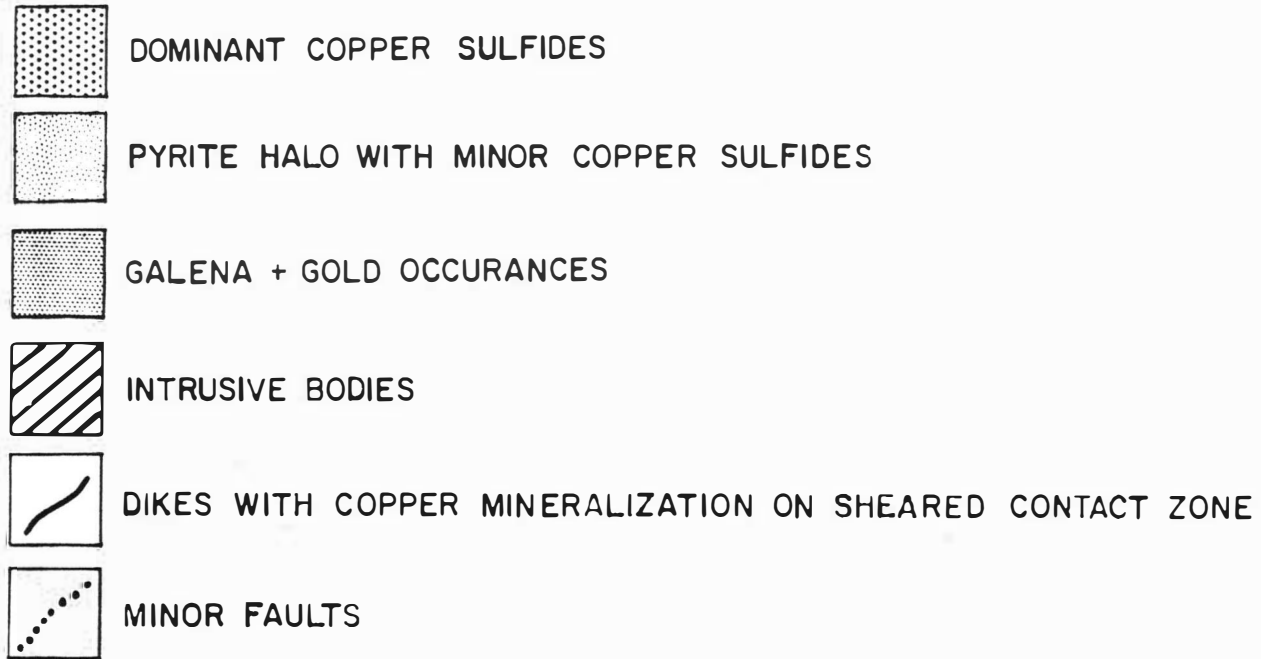


Figure 8. Legend for the Kennecott map of mineralization.

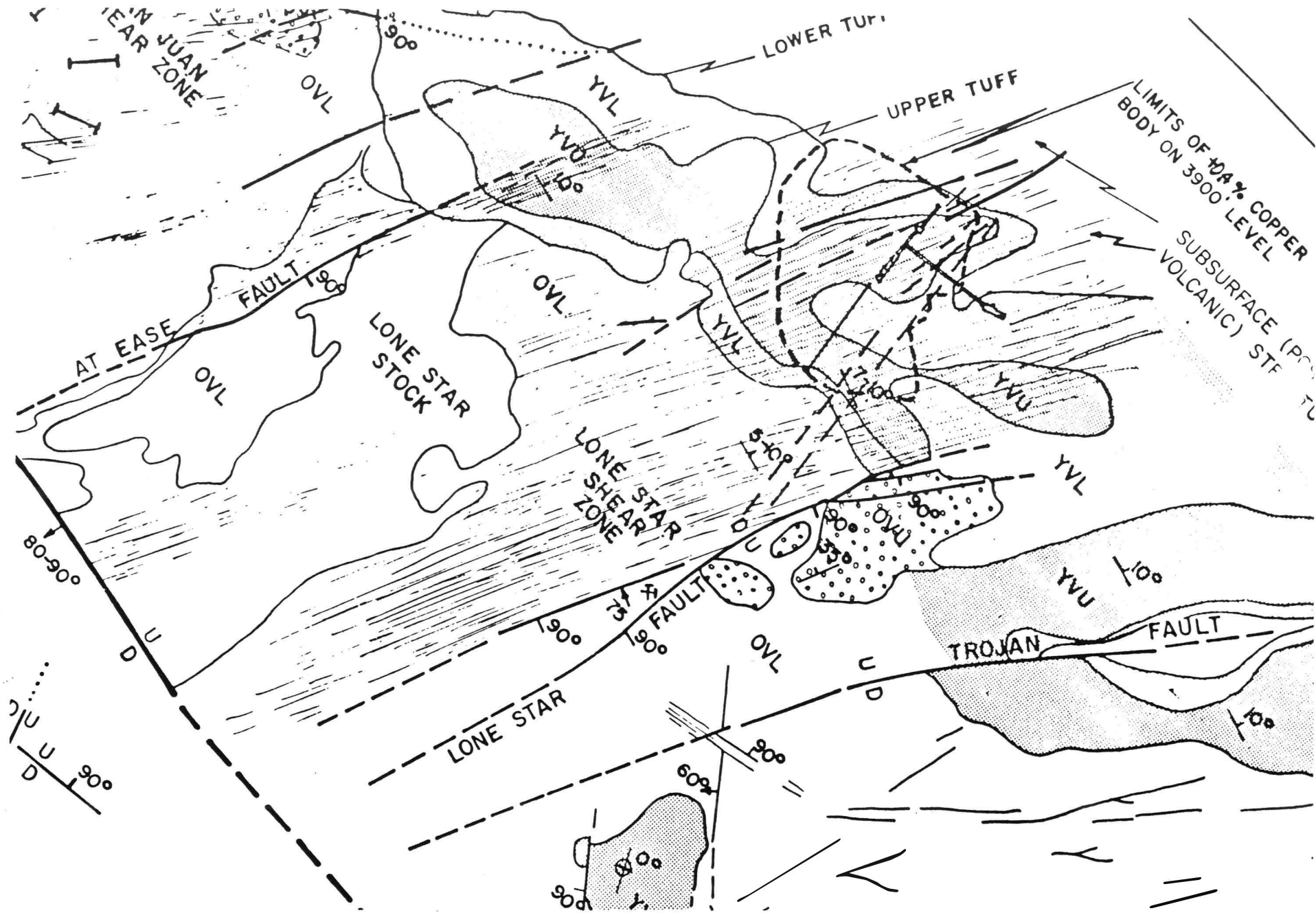


Figure 9. Structural map, vicinity of the Kennecott deposit (courtesy of the Kennecott Corp.)

LEGEND






YVU	UPPER UNIT YOUNGER VOLCANICS
YVL	LOWER UNIT
IV	INTERMEDIATE VOLCANICS
OVU	UPPER UNIT OLDER VOLCANICS
OVL	LOWER UNIT
	SHEAR ZONES WITH IMPORTANT COMPLEMENTARY ELEMENTS
	FAULTS OBSERVED, PROJECTED, INFERRED
	FRACTURE ZONE DEFINED BY D. KING AND SHEARING
	ATTITUDE OF VOLCANIC UNITS
	CONTACT OBSERVED, INFERRED

Figure 10. Legend for the Kennecott structural map, Figure 9



Figure 11. Enlarged portion of a NASA color aerial photograph of the Kennecott area at 1:24,000 scale.



Figure 12. Simulated Thematic Mapper image of the Kennecott area at 1:24,000 scale. This is a canonical transform image processed by the Jet Propulsion Laboratory from NASA NS-001 airborne scanner data (courtesy of the Geosat Committee, Inc.).

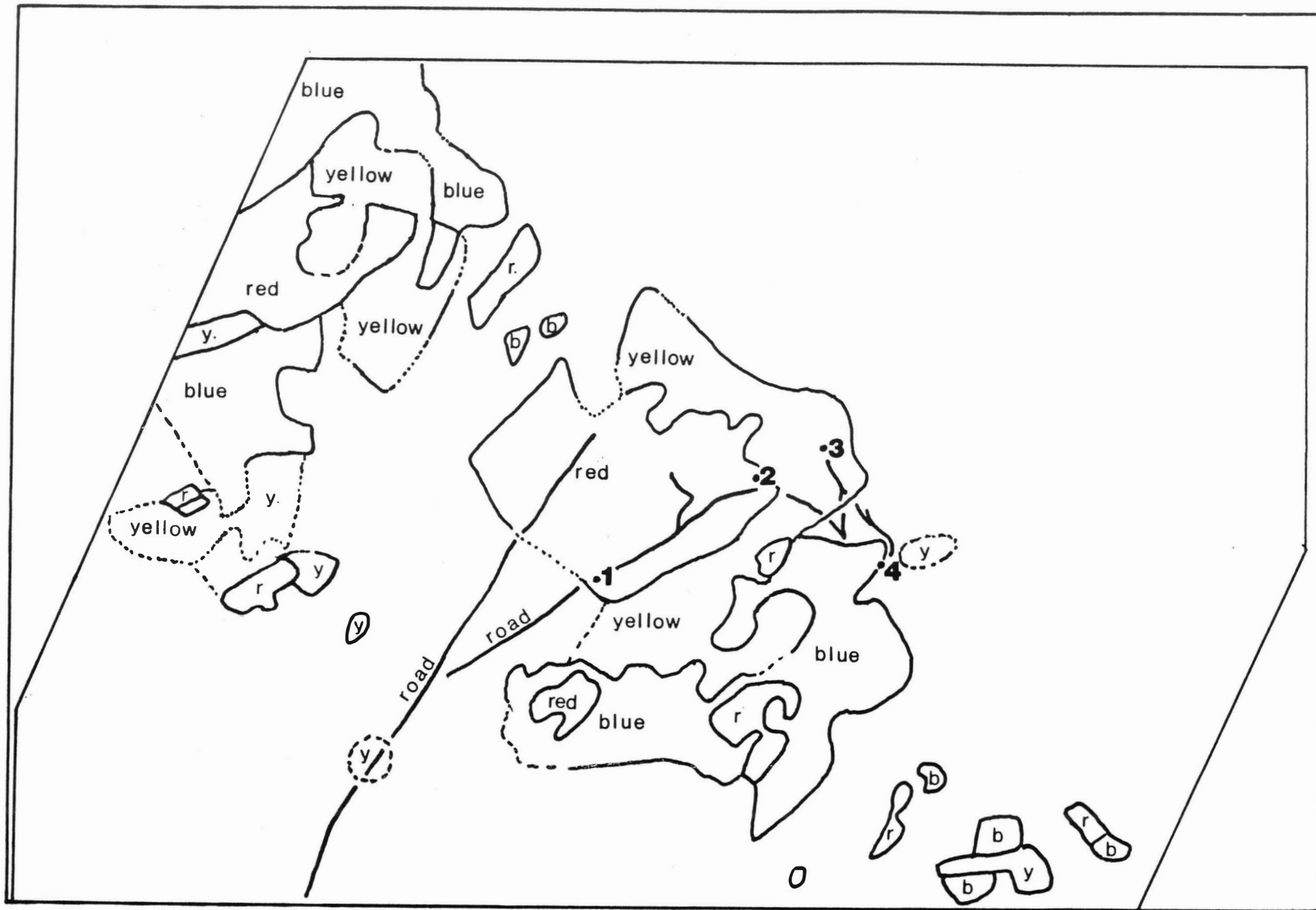


Figure 13. Map of spectral anomalies, derived from the canonical transform image, indicating areas of suspected phyllic alteration. The location of samples taken reflectance spectra and mineralogic analysis shown by numbers 1,2,3, and 4.

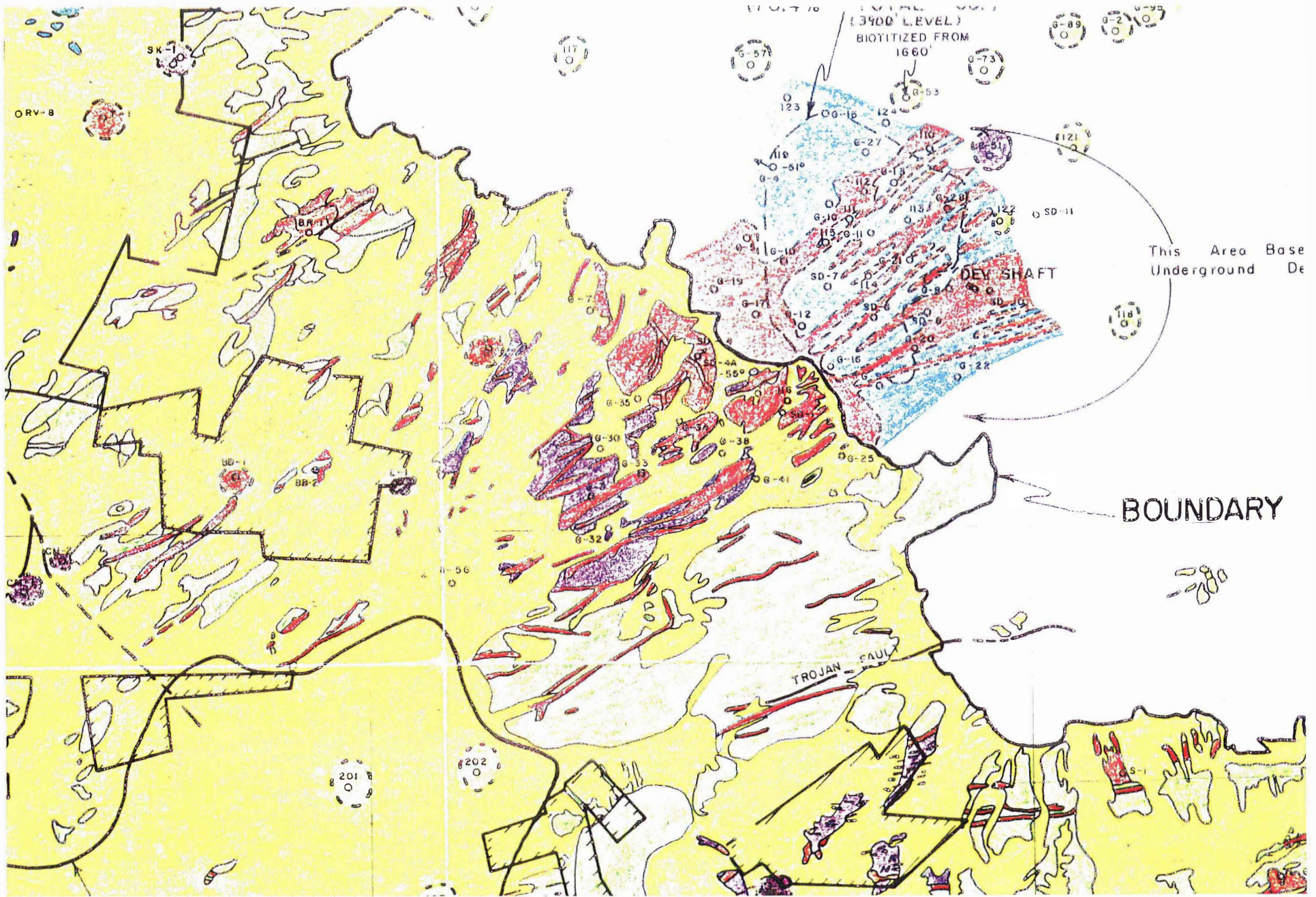


Figure 14. Alteration map, vicinity of the Kennecott deposit, 1:24,000 scale (courtesy of the Kennecott Corp.).

—LEGEND—

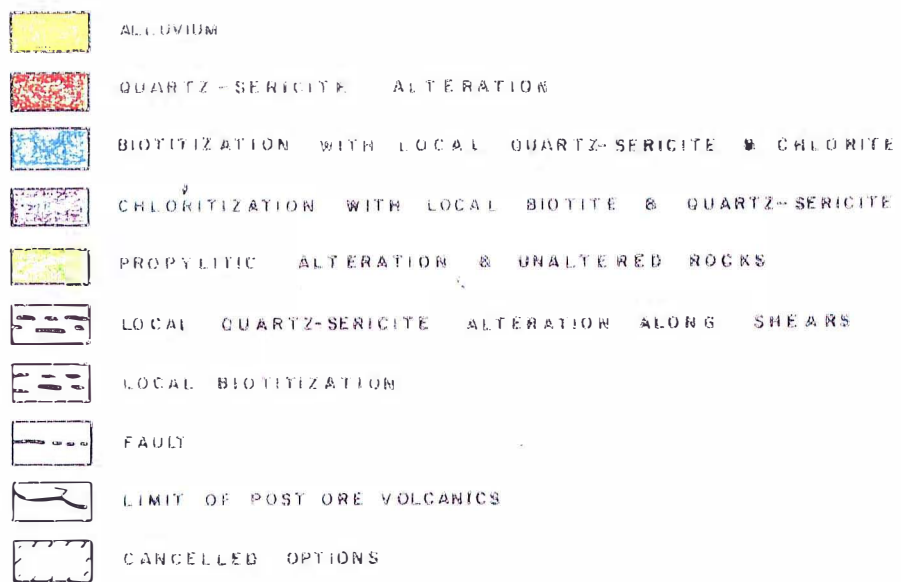


Figure 15. Legend for the Kennecott alteration map.



Figure 16. Enlarged portion of a NASA color aerial photograph of the Dos Pobres area, approximately 1:10,000 scale.

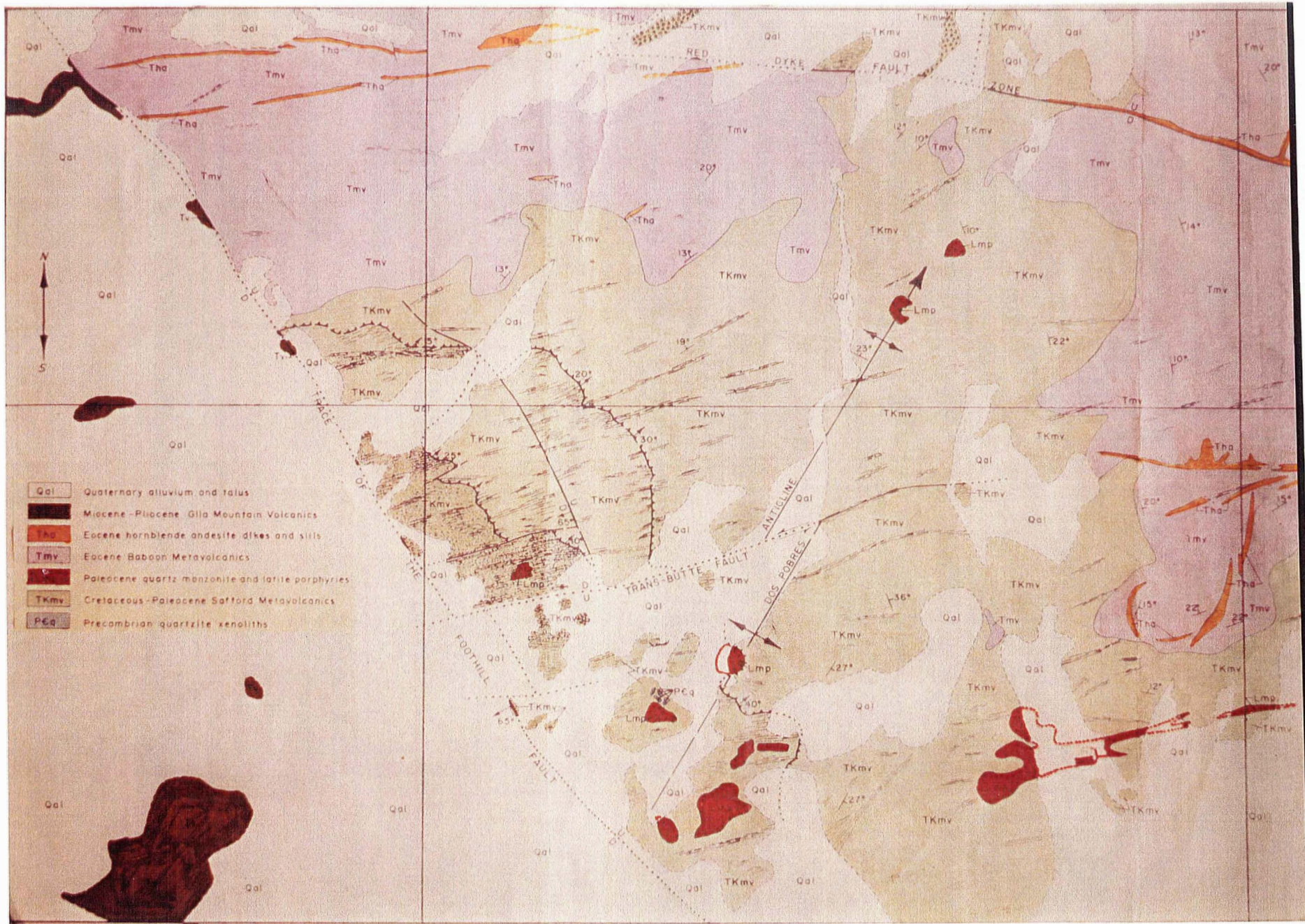


Figure 17. Geologic map of the vicinity of the Dos Pobres Orebody, approximately 1:10,000 scale (courtesy of the Phelps Dodge Corp; also in Langton and Williams, 1982). Stipples indicate pervasive biotite alteration and disseminated cuprite - chrysocolla.

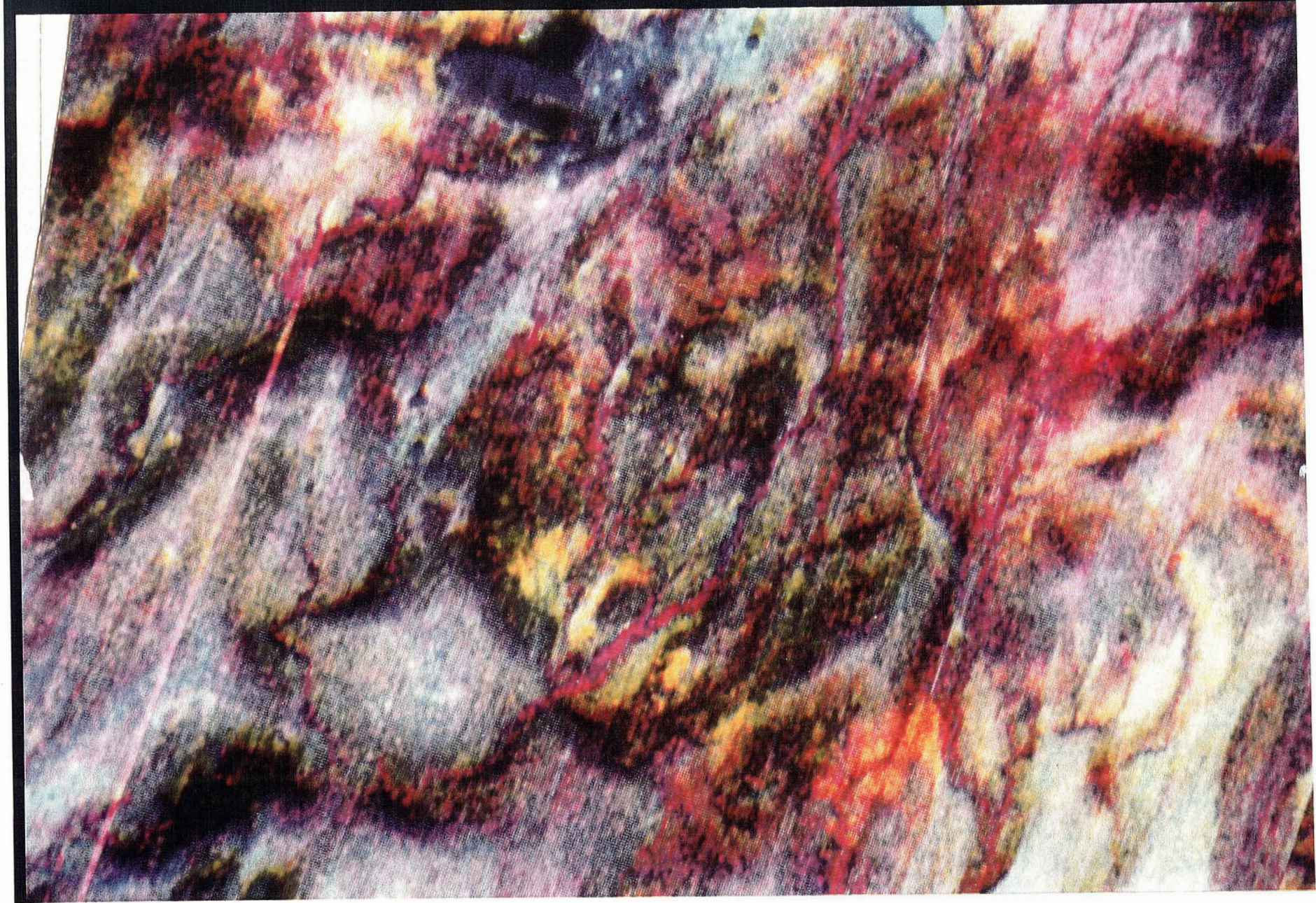


Figure 18. Thematic Mapper Simulator image, three-ratio color composite image processed by Jet Propulsion Laboratory from NASA NS-001 multispectral data (courtesy of the Geosat Committee, Inc.)

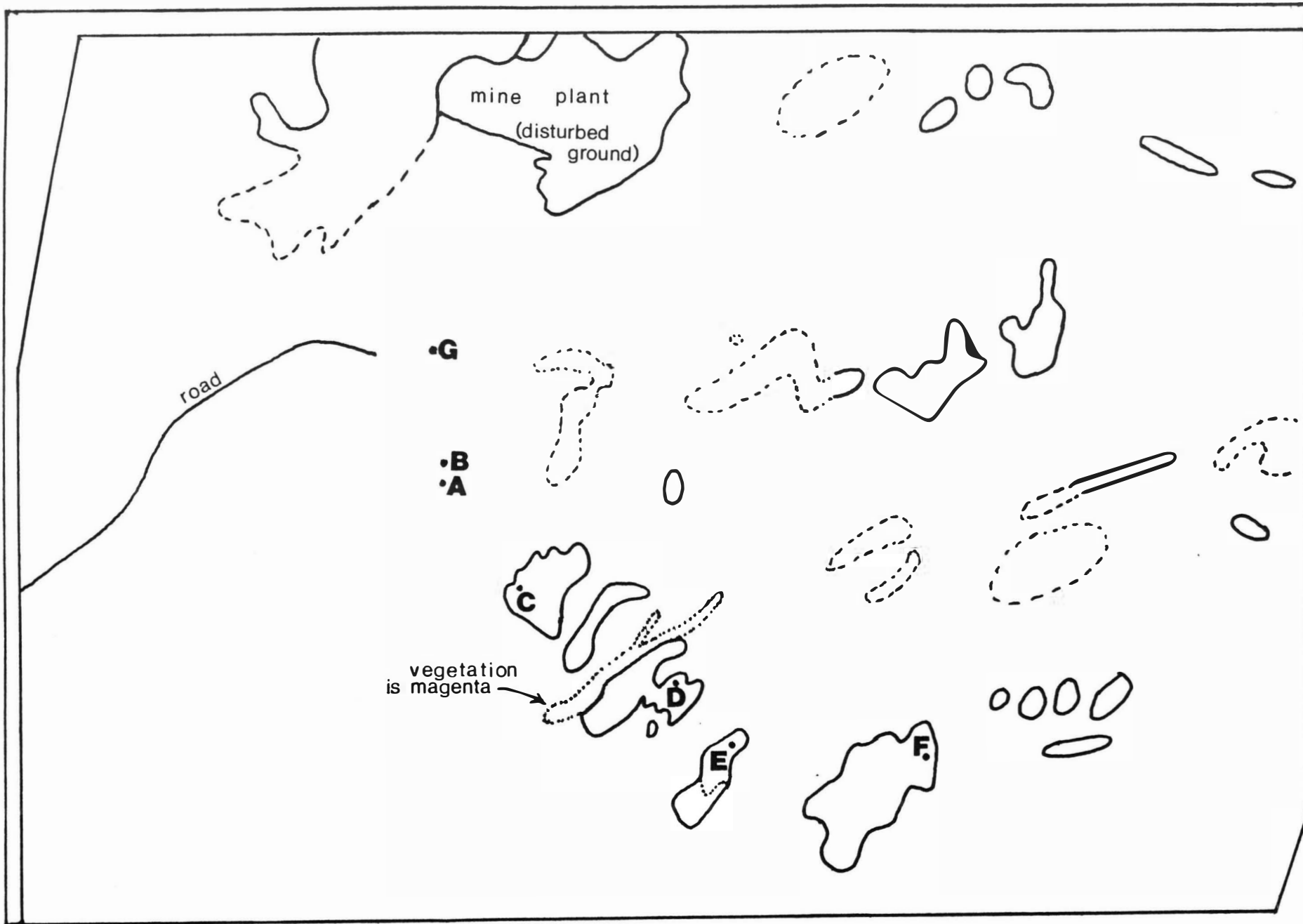


Figure 19. Map of spectral anomalies derived from the three ratio image, indicating areas of suspected phyllic alteration and the location of rock samples taken for analysis.

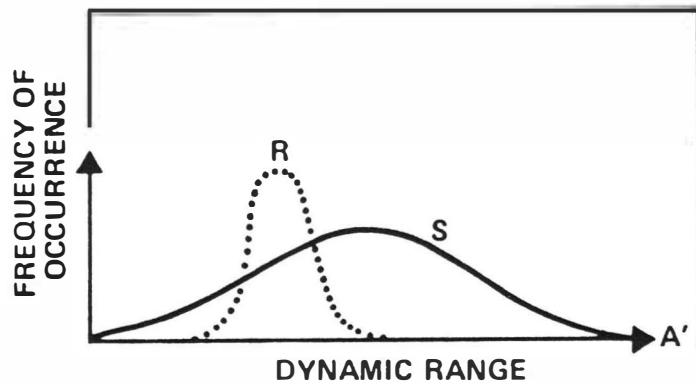


Figure 20. Schematic drawing of a linear contrast stretch performed on a digital data set. The total dynamic range of a film recorder system is represented by the distance A-A' along the abscissa. The original raw data as received from the sensor system are depicted by the curve R, whereas the resultant stretched data, with scaling and translation, are shown by curve S. Curve S now occupies the total dynamic range of the film. Other types of stretches can be tailored to the data and the requirements of the output image.

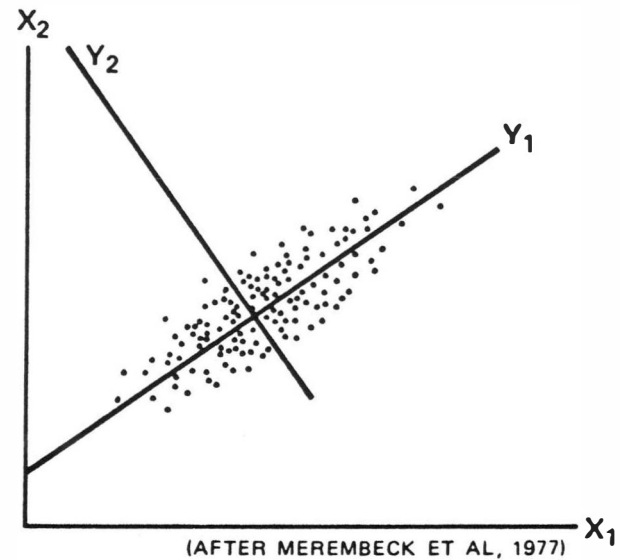


Figure 21. Elliptical scatter pattern for a hypothetical data set consisting of multi-spectral channels X_1 and X_2 . The principal component analysis creates a new set of coordinate axes (components) by a rotation and translation such that the first (Y_1) component accounts for most of the variability. The second axis (Y_2) is chosen orthogonal to the first. This concept can be extended to multidimensional space, with each succeeding component axis being oriented orthogonal to the earlier ones and accounting for less and less variation.

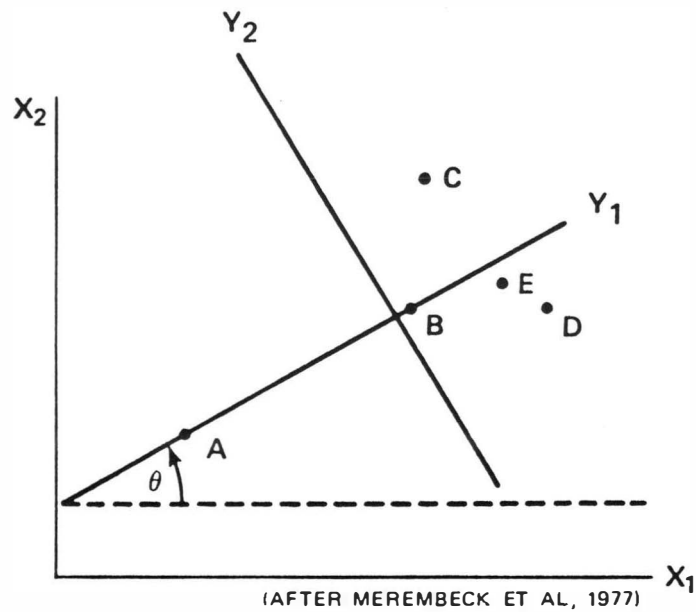


Figure 22. Mean values (depicted by center-points) and density distribution (depicted by the ellipses) for hypothetical categories A through E. Axes X_1 and X_2 depict the original data channels. Note that on the basis of axis X_1 , categories A-B-D are separable; categories A-B-C are separable on X_2 . Categories B-C-E and D-E are not separable on X_2 . Based on both X_1 and X_2 category E is confused with B and D.

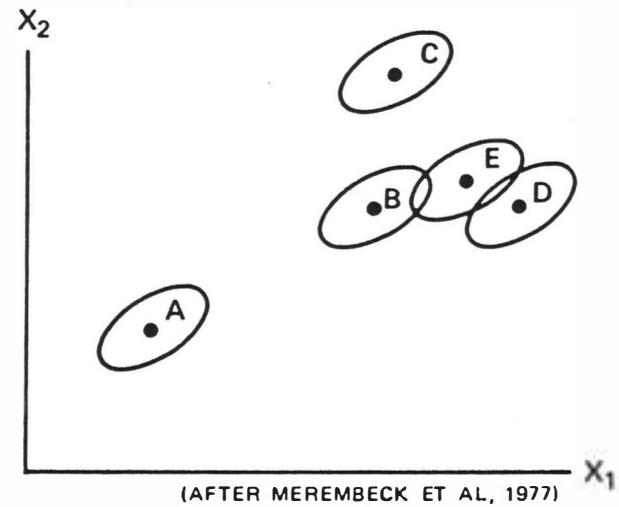
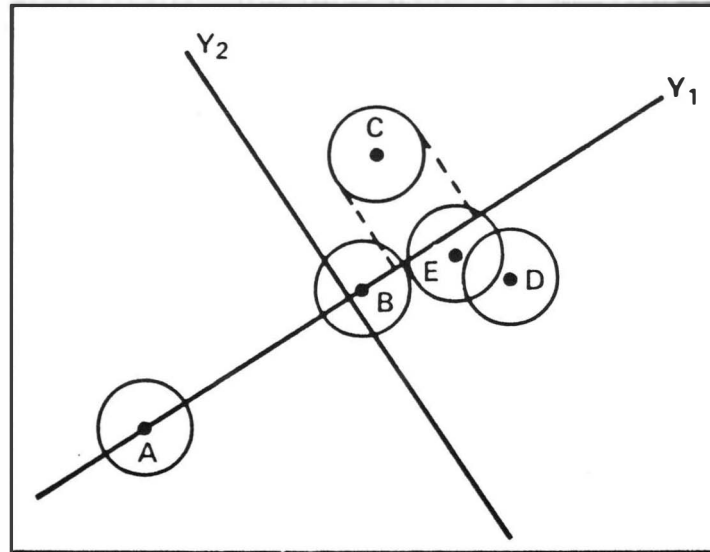
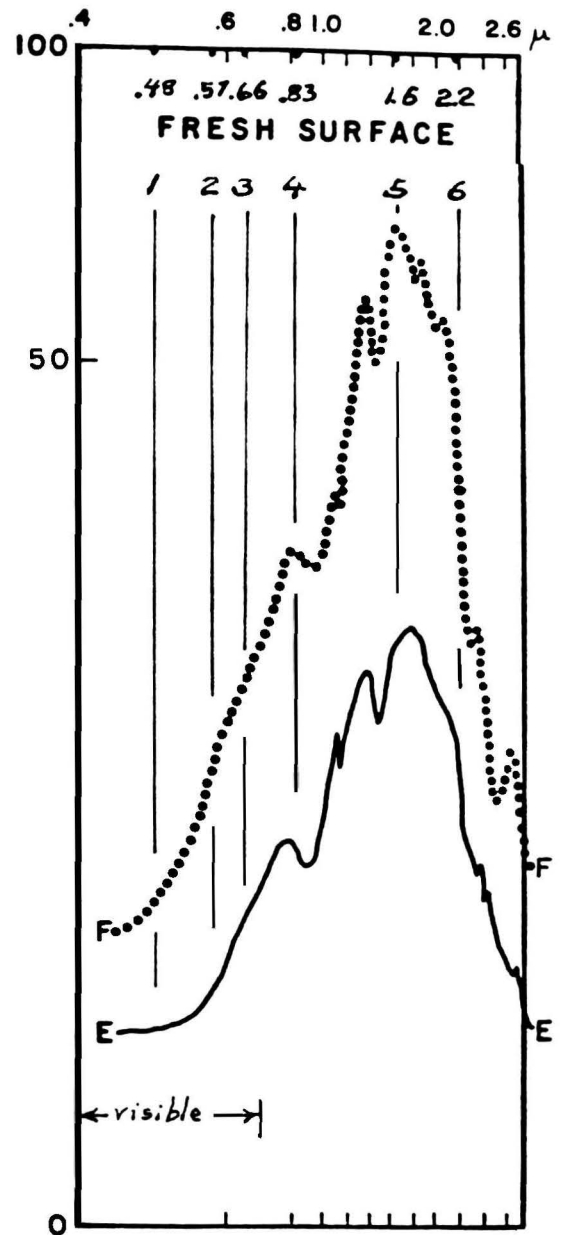
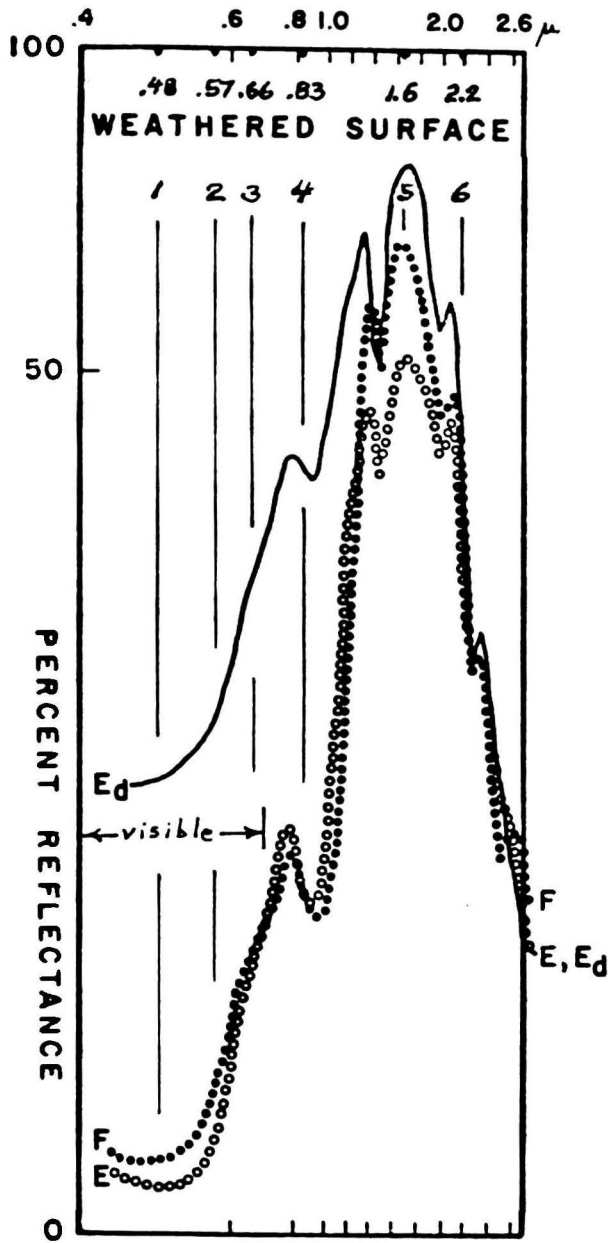


Figure 23. Canonical transformation involving rotation (θ) and translation for categories A through E. Axes Y_1 and Y_2 respectively depict the first and second transformed axes.

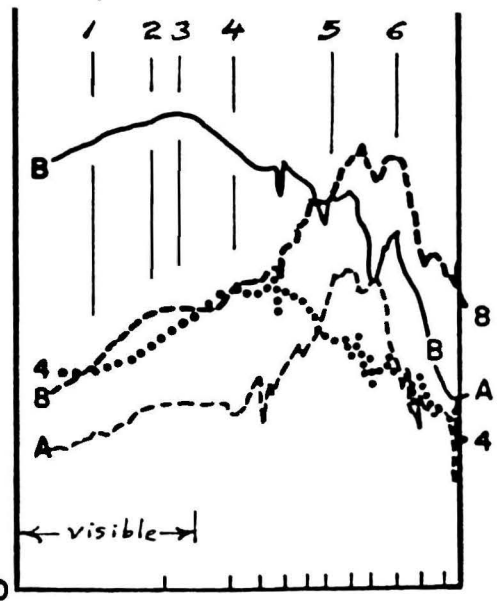
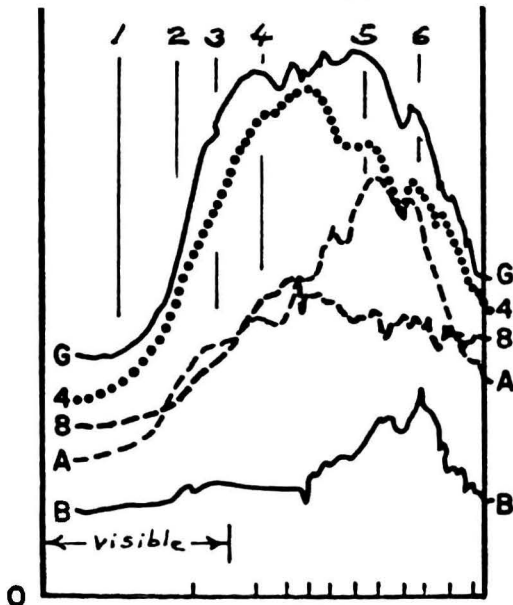


(AFTER MEREMBECK ET AL, 1977)

Figure 24. Canonical rotation, translation and scaling transformation showing separability between categories A through E. The transformed axes Y_1 and Y_2 have been scaled so that the previously elliptical density distributions are now spherical (i.e., units on $Y_1 \neq Y_2$). Based on axis Y_1 , category A is separable from all other categories. Categories B-E and B-D are separable. Categories B-C and C-D-E are confused. Based on axis Y_2 , C is separable from all others. Categories A-B-D-E are confused. Only categories D-E cannot be separated on the basis of the two axes; this is an improvement over the original data.



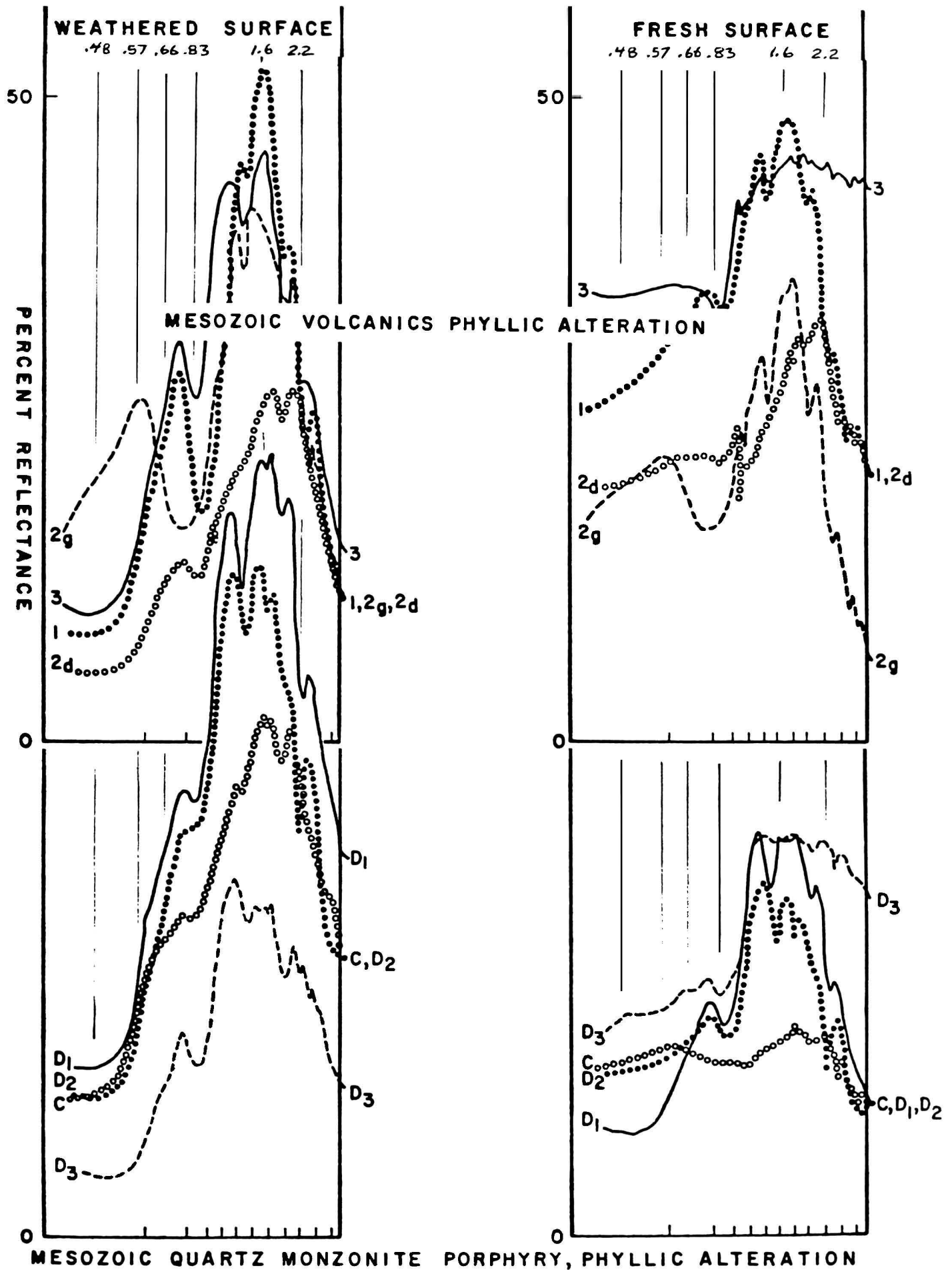
MESOZOIC QUARTZ MONZONITE PORPHYRY, ARGILLIZED



MESOZOIC ANDESITE PROPYLITIC ALTERATION

Figure 25. Reflectance spectra of host rocks, showing positions of Thematic Mapper bands. Note the contrast between argillized (phyllitic) rocks and propylitically altered rocks.

Figure 26. Reflectance spectra of host rocks. Note the difference between spectra of weathered and fresh rock surfaces.



Preprint from:

Proceedings of 2nd IEEE International
Geology and Remote Sensing Symposium
(IGARSS), Munich, Germany June, 1982

LANDSAT-D TM APPLICATION TO PORPHYRY COPPER EXPLORATION

Michael Abrams, Jet Propulsion Laboratory, California Institute of Technology,
Pasadena, CA 91109
David Brown, Texasgulf, Tucson, AZ 85711
Larry Lepley, Tucson, AZ 85704
Ray Sadowski, AMAX, Tucson, AZ 85701

ABSTRACT

Data from the current Landsat scanners were compared with data acquired with an aircraft instrument simulating the new Landsat-D Thematic Mapper (TM) scanner. Three porphyry copper deposits were used as test sites to evaluate the spatial and spectral capabilities of both systems for separation of lithologies, discrimination of hydrothermal alteration, and structural mapping.

Landsat data were useful for delineating iron oxide areas on the surface, some of which were associated with altered rocks, some of which were associated with sedimentary redbeds, volcanic rocks, and weathered alluvium. The limited spatial resolution hampered the ability to map critical geologic relationships. The simulated TM data provided additional spectral bands and improved spatial resolution which allowed several types of alteration to be discriminated, and the important geologic features to be mapped.

The Landsat-D TM scanner will provide geologists with an improved mapping tool, applicable not only to porphyry copper exploration, but also to exploration for a wide range of base and precious metal deposits.

Keywords: Remote sensing; copper exploration; Landsat-D; Thematic Mapper

1. INTRODUCTION

Landsat data have been used for a number of years in arid to semi-arid environments to locate areas of iron oxide occurrences which might be associated with hydrothermal alteration zones. Pioneering work by Rowan and his coworkers (Ref. 1) clearly demonstrated the utility of computer processing of Landsat data to locate alteration zones in Nevada associated with precious metal deposits. However, iron oxides have a wide range of occurrences often unrelated to alteration phenomena; these include sedimentary redbeds, volcanic rocks, weathered alluvium, etc. In addition there are areas of alteration which are iron oxide-free, such as advanced argillic, silicic, and sulfataric alterations. These areas are characterized by the presence of hydrous minerals, such as kaolinite, alunite, and sericite. The spectral information provided by the current Landsats does not allow detection of

these areas, and fails to distinguish many unaltered areas from altered areas. Another drawback of Landsat is its relatively poor spatial resolution (80 m) which prevents recognition of moderate to small features and outcrops which might be of critical importance.

The fourth Landsat, scheduled to be launched in July, 1982 will carry a new generation multispectral scanner called the Thematic Mapper (TM). This instrument will have 7 channels and provide data with 30 m spatial resolution (Table 1).

TABLE 1. SPECTRAL BANDS OF LANDSAT MSS AND LANDSAT-D TM

Landsat MSS		Landsat-D TM	
Band	Wavelength	Band	Wavelength
4	0.5-0.6	1	0.46- 0.50
5	0.6-0.7	2	0.52- 0.60
6	0.7-0.8	3	0.63- 0.69
7	0.8-1.1	4	0.76- 0.90
		5	1.55- 1.75
		6	2.08- 2.36
		7	10.8 -12.50

Two of the spectral channels (1.6 μ m and 2.2 μ m) are located in wavelength regions which should allow detection of hydrous minerals, as well as iron oxides using data from the other bands.

To examine the applications of Landsat-D TM data for copper exploration, Landsat data were compared with simulated TM data acquired using an aircraft scanner instrument. Three porphyry copper deposits in Arizona were selected for investigation: Silver Bell, Safford, and Helvetia. These sites present a range of copper occurrences in semi-arid environments, with different host rocks, levels of erosion, and stages of development. Both sedimentary and igneous terrains are represented; the varying levels of erosion provide exposures of alteration phenomena from the most intense potassic to regional propylitic.

2. ANALYSIS OF LANDSAT DATA

Landsat data provided some information on alteration at all three sites. Using a color ratio composite of band ratios 4/5, 5/6, and 6/7 areas with iron oxides present at the surface were identifiable at all sites. These areas include both altered rocks, and iron-rich unaltered

rocks. At Silver Bell, iron oxides associated with the phyllic alteration zone along the Silver Bell fault zone were identifiable. Other, unaltered areas have a similar appearance on the images, including sedimentary redbeds and limonitic Precambrian granites. A few rock types were separable, but the limited spatial and spectral resolution made discrimination of many rock types impossible. At Safford, iron oxide areas associated with two copper deposits were identifiable; additional areas of iron oxide corresponding to weathered alluvium and gravels appeared similar. At Helvetia, altered hematitic arkose was discernible as were areas of unaltered volcanic sediments. Again, the poor spatial and spectral resolution provided only limited geologic information.

3. ANALYSIS OF FIELD SPECTRAL DATA

In order to examine the expected improvement provided by the Landsat-D TM spectral data, field reflectance measurements were obtained using JPL's Portable Field Reflectance Spectrometer (PFRS) at the three test sites. Most of the major rock types at the sites were measured in the wavelength region of 0.45 to 2.45 μm . Statistical analyses of the spectra were performed using a stepwise linear discriminant analysis program. The program was provided groups of rock spectra, and various wavelength regions from the PFRS data simulating several scanners. The program determines the optimal linear combination of the wavelength variables to separate the rock-type groups. A comparison of the separability of groups from each of the test sites for Landsat and simulated Landsat-D TM data is shown in Table 2.

TABLE 2. CLASSIFICATION ACCURACY OF SIMULATED LANDSAT DATA VS. SIMULATED TM DATA

Site	No. Groups	Landsat	TM	Improvement
Safford	12	46%	65%	19%
Helvetia	10	50%	68%	18%
Silver Bell	10	65%	89%	24%

In all three test sites, TM data provided an increase of about 20% in correctly identified sampled rock groups.

A second test was performed to compare the TM scanner and a conceptual scanner with 30 equally spaced 0.05 μm wide bands in the 0.45-2.45 μm region. The stepwise discriminant analysis program surveyed the 30 bands and selected, in order of importance, those bands which best separated the rock groups. The order of band selection for the TM and the 30 channel simulation for the same rock groups is shown in Table 3.

TABLE 3. ORDER OF BAND SELECTION FOR TM AND 30 CHANNEL SIMULATIONS USING TEST SITE PFRS DATA

Silver Bell		Helvetia		Safford	
TM*	30*	TM	30	TM	30
1.65	1.60	0.48	0.50	2.22	2.15
2.22	2.15	0.66	0.70	1.65	2.20
0.48	0.50	1.65	1.70	0.83	0.50
0.56	0.55	0.56	2.30	0.56	2.05
0.66	0.70	0.83	2.20	0.66	0.90
0.83	0.60	2.22	2.05	0.48	1.55

*Center wavelengths of bands, in microns

The Silver Bell analysis exhibits a nearly one-

to-one correlation in both the order of band selection and the particular bands selected. From a statistical standpoint, the TM bands are ideally chosen for discriminating the suite of altered and unaltered rocks sampled at Silver Bell. The Helvetia analysis shows similar behavior for the first three bands (the most important selected by the discriminant function program). A somewhat poorer correlation exists for the Safford analysis; however, the 0.5, 2.2, 1.55, and 0.9 μm regions were selected in the 30 channel analysis as the most important. These match fairly closely some of the channels of the TM.

4. THEMATIC MAPPER SIMULATOR AIRCRAFT DATA

Thematic Mapper data were obtained with NASA's NS-001 TM simulator aircraft scanner. Data were obtained from an altitude of 5 km, producing a 10 km swath width with a resolution of about 12 m. This scanner has the same 7 bands as the TM, and an additional band at 1.0-1.3 μm .

In order to examine detection of hydrothermal alteration, a color ratio composite was produced for each of the three sites using TM band ratios 3/2 (0.66 μm /0.56 μm), 4/5, and 5/6 (1.6 μm /2.2 μm). These particular ratios were chosen to enhance the presence of iron oxide minerals and hydrous minerals. The 3/2 ratio will be high for iron oxides due to the fall-off in reflectance towards the ultraviolet. Hydrous minerals will have a high 5/6 value due to the absorption band near 2.2 μm caused by OH⁻. This particular combination was shown to be effective for discriminating hydrothermal alteration of an epithermal precious metal deposit in Nevada (Ref.2).

At Silver Bell, the phyllic alteration zone was clearly delineated. Comparison with an alteration map produced from months of field and laboratory work showed a nearly perfect correlation. This zone was distinguishable due to spectral features of the mineralogical constituents. Iron oxides (goethite, hematite) developed on the surface from oxidation of hydrothermal pyrite, and kaolinite and sericite produced from alteration of feldspars have diagnostic and strong absorption features in the TM wavelength bands. Sedimentary redbeds and other ferruginous, unaltered rocks were distinguishable from altered rocks due to their lack of hydrous minerals.

At Safford, sericitic alteration associated with the copper deposits showed up clearly for the same reasons as at Silver Bell. The altered rocks were a quartz monzonite intrusive, and rhyolitic dikes along a shear zone. At Helvetia, a large hematitic area east of the ore body was visible. This area has pervasive hematite developed from oxidation of hydrothermal pyrite. Argillic alteration was discernible over an outcrop of the mineralizing quartz latite porphyry.

The NS-001 TM data were also processed using stepwise linear discriminant function analysis. The ground spectral reflectance measurements provided the training sets to calculate the optimal linear combination of wavelength bands to separate the rock groups examined. (See Ref. 3 for a complete discussion.) For Silver Bell, analysis of the images produced from the new linear combinations indicated that all the mapped geologic

units could be distinguished. In addition, some of the mapped units appeared in different colors, corresponding to phyllic and propylitic alteration, and unaltered rocks. These data were degraded to the Landsat-D resolution of 30 m; little information was lost compared to the original 12 m data. Major dikes were visible, allowing structural information to be extracted; all outcrops were separable.

Similar processing was performed on the Safford and Helvetia data, with equally successful results. At Helvetia, unaltered limestones were separable from altered limestones (marbles) related to skarn development. The overall improvement compared to current Landsat data was striking.

5. IMPLICATIONS FOR MINERAL EXPLORATION IN GENERAL

Porphyry copper deposits are characterized by several features which are common to other types of deposits. These are: structural control, hydrothermal alteration zones, and presence of a mineralizing intrusive. Hydrothermal alteration zones are due to the physicochemical reactivity of magmatic and/or meteoric fluids which are associated with intrusive or extrusive bodies. Circulating fluids change the mineralogy of the country rocks and can produce distinctive and diagnostic assemblages. The zoned alteration sequence developed in association with porphyry copper deposits is a classic example of this interaction. Mineralizing fluids are generated by and from the intrusive body. Alteration is most intense closest to the intrusive, and decreases in intensity away from the intrusive.

There are many other types of deposits which share some or all of these features. The techniques developed in this study using TM data should be directly applicable to deposits which occur in similar climatic zones (arid to semi-arid). These deposits include:

1) Hypothermal deposits which contain ores of Au, Sn, Mo, W, Cu, Pb, Zn, As; alteration can include sericitization in siliceous rocks, and chloritization; examples are Au of Kirkland Lake, Ontario and Kalgoorlie, W. Australia; Sn of Cornwall.

2) Mesothermal deposits which include porphyry coppers; they form in or near intrusive igneous rocks, and contain ores of Au, Ag, Cu, As, Pb, Zn, Ni, Co, W, Mo, U; alteration includes sericitization, argillization, propylitization, carbonitization. Other porphyry type deposits are associated with molybdenum, tin, and gold mineralization. The results of this study should be directly applicable to exploration for these types of deposits. Porphyry molybdenum deposits differ from copper deposits only in the dominant ore minerals and the wetness of the intrusive. As a result, alteration zones are spatially more restricted and often telescoped. Nevertheless, phyllic, quartz-sericitic, argillic, and propylitic alteration zones are common and diagnostic. Tin and gold deposits do not develop the intensity of alteration seen at copper and molybdenum deposits. Nevertheless, argillic and propylitic alterations are common, and can be looked for.

3) Epithermal deposits; these form near surface and are associated with extrusive or near surface

intrusive rocks; they contain ores of Pb, Zn, Au, Ag, Hg, Sb, Se, Bi, U; alteration can be sericitization, argillization, kaolinization, and dolomitization; examples are Au of Goldfield, Nevada; Comstock, Nevada; Ag of Tonopah, Nevada. Previous work (Ref.2) at these Nevada locations has demonstrated the power of the Thematic Mapper bands for mapping alteration facies. In the Goldfield area five different types of alteration were separable: intense argillic, silicification, opalization, opalization with iron-oxides, and deuteric. These results should be extendable to other vein deposits and epithermal systems where alteration is present.

6. CONCLUSIONS

Simulations of Landsat-D TM data using aircraft scanners indicate:

1) The added spectral bands of the TM compared to current Landsat scanners will provide more useful information for lithologic mapping and mapping of hydrothermal alteration associated with porphyry copper deposits. The presence of bands in the 1.6 and 2.2 μ m regions proved to be invaluable for identifying areas of hydrothermal alteration due to their sensitivity to the presence of hydrous minerals.

2) The improved spatial resolution of Landsat-D TM (30 m) versus that of the current Landsat (80 m) allows detection of outcrop areas and geologic features critical for geologic mapping. This was evident from analyses and comparisons of data at 80 m, 30 m, and 12 m for Silver Bell. Little information was lost going from 12 m to 30 m, compared to the limited information visible on the 80 m data.

3) The new Landsat-D TM scanner will provide exploration geologists with a new improved mapping tool for surveying mineral resources on a global basis. Although this study was limited to examination of porphyry copper deposits, the similarity of mineralogical assemblages and alteration zones associated with many other types of base and precious metal deposits suggests that TM data will have wide application for the non-renewable resource exploration community.

7. REFERENCES

1. Rowan L C et al 1974, Discrimination of Rock Types and Altered Areas in Nevada by the use of ERTS Images, U.S. Geological Survey Professional Paper 883, 35 pp.
2. Abrams et al 1977, Mapping of hydrothermal alteration in the Cuprite Mining District, Nevada using aircraft scanner images for the spectral region 0.46 to 2.36 μ m, Geology Vol. 5, 713-718.
3. Abrams et al 1982, The Joint NASA/Geosat Test Case Project, JPL Technical Report, Jet Propulsion Laboratory, Pasadena, CA, in press.

The research described in this paper was carried out as part of the Joint NASA/Geosat Test Case Study by the Jet Propulsion Laboratory, California Institute of Technology, under contract with the National Aeronautics and Space Administration; and by geologists of U.S. mineral and petroleum exploration companies under the auspices of the Geosat Committee, Inc.

FIELD TRIP ATTENDEES
AGS SPRING FIELD TRIP 1982

Steve Applebaum
Phelps Dodge
P. O. Drawer 1217
Douglas, AZ 85607

Dr. Charles C. Bates,
Consultant
P. O. Box 191
Green Valley, AZ 85614

Dave Boggess
Phelps Dodge Corp. Morenci Branch
109 Maricopa St., Morenci, AZ

Jim Briscoe & Tom Aldrip
Westland Minerals Exploration Co.
5701 E. Glenn #120
Tucson, AZ 85712

J. L. Christman
Exxon Minerals Co.
P. O. Box 739
Silver City, NM 88062

Dr. Radu Ciocavelea
Billiton Exploration, USA Inc.
4633 E. Broadway, Ste 123
Tucson, AZ

Thomas Conto
Inspiration Development Co.
P. O. Box 1320
Claypool, AZ 85532

Annan Cook
Consulting Geologist
942 Wanda Vista Place
Tucson, AZ 85704

Fred Craxen
Arizona Western College
Yuma, AZ

Melinda Cuff
Az. Western College
Yuma, AZ

Darrel Dean
Exxon Minerals Co.
P. O. Box 739
Silver City, NM 88062

Chuck Douthitt
Exxon
2425 N. Huachuca Dr., Ste A,
Tucson, AZ 85745

Jonathan Duhamel
Phelps Dodge Corp.
P. O. Drawer 1217
Douglas, AZ 85607

Peter Dunn
Chevron Resources, Inc.
P. O. Box 36674
Tucson, AZ 85740

David Emmons
Tenneco
3755 E. 34th St., Ste 103,
Tucson, AZ 85713

Larry Fellows
AZ. Bur. of Geology & Min. Tech.
845 N. Park Ave., Tucson, AZ 85719

William C. Feyersbend
Gold Fields Mining
Box 329
Yuma, AZ 85364

Lera R. Gates
4410 Camino Kino
Tucson, AZ 85718

Jim Hoopes
Chevron Resources
P. O. Box 36674
Tucson, AZ 85740

Holly Huyck
Lakeshore Mine
Casa Grande, AZ

Kristie Jennings
Az. Western College
Yuma

Fleetwood R. Koutz
ASARCO INC. - SW Expl. Div.
Box 5747
Tucson, AZ

Henry G. Kreis
ASARCO INC.
P. O. Box 5747
Tucson, AZ

Mario R. Lluria
Exxon Minerals Co.
2425 N. Huachuca Ave.
Tucson, AZ 85745

James Loghry
Consulting Geologist
2121 E. Monte Vista Dr.
Tucson, AZ 85719

Stephen A. Langford
9140 N. Shadow Mountain Dr.
Tucson, AZ 85704

L. K. Lepley
Consultant
8841 N. Calle Loma Linda
Tucson, AZ

J. David Lowell
Pillar, Lowell & Assoc.
5115 N. Oracle Road
Tucson, AZ 85704

John Maddry
Tennelo
3755 E. 34th St., Ste 103,
Tucson, AZ 85713

Peter Mesard
Exxon Minerals Co.
P. O. Box 739
Silver City, NM 88062

Syver W. More
Billiton Exploration, USA, INC.
4633 E. Broadway, Suit #123
Tucson, AZ 85711

G. W. Pickard
ASARCO, INC.
1150 N. 7th Ave.,
Tucson, AZ 85703

Jack Pigott
St. Joe American Corp.
2002 N. Forbes Blvd., #108
Tucson, AZ

Chris Pointon
Villiton International Metals B.V.
19 Louis Couperusplein, 2514 HP
P. O. Box 190, 2501AS
The Hague, The Netherlands

Richard K. Preece
Phelps Dodge Corp.
Geology Dept.
Phelps Dodge Corp.
Morenci, AZ 85540

Kenyon Richard
Consultant, Mining Geology
11 Orange Grove Rd., Apt. 535
Tucson, AZ 85704

Niles G. Shaki
Utah International Inc.
7840 E. Broadway, suite 209
Tucson, AZ 85710

Francis Sousa
St. Joe American Corp.
2002 N. Forbes Blvd. #108
Tucson, AZ 85705

Claudia Stone
Bureau of Geology
2045 N. Forbes Blvd. #106
Tucson, AZ 85705

William J. Thomas
Retired-Phelps Dodge Corp.
Box 202
Ajo, AZ

Tom Waldrip
Westland Minerals Exploration
5701 E. Gleen #120
Tucson, AZ 85712

Dennis Watt
AZ. Western College
Yuma

D. Edward Wells
Inspiration Devl. Co.
P. O. Box 1320
Claypool, AZ 85532

Waldo Cuadra
Shell Chili
Casilla 4 Correo 9 Avenida
Providencia 1979 10^o Piso
Santiago, Chili

Rupert Scheuplein
Shell Chili
Casilla 4 Correo 9
Avenida Providencia 1979 10^o Piso
Santiago, Chili

AGS THANKS THE FOLLOWING COMPANIES FOR CONTRIBUTIONS
TO THIS FIELD TRIP:

Union Molycorp
Cities Service
Newmont Exploration